NiII complex supported by an iminophosphorane ONP ligand: Synthesis and catalytic C=C and C=O bonds hydrosilylation

Ingrid Popovici, Thomas F Arkwright Arcilla, Sophie Bourcier, Nicolas Casaretto, Vincent Gandon, Audrey Auffrant

Ni^{II} complex supported by an iminophosphorane ONP ligand: Synthesis and catalytic C=C and C=O bonds hydrosilylation

Received 00th January 20xx,
Accepted 00th January 20xx

DOI: 10.1039/x0xx00000x

Ingrid Popovici,[a] Thomas F. Arkwright Arcilla,[a] Sophie Bourcier,[a] Nicolas Casaretto,[a] Vincent Gandon,*[b] and Audrey Auffrant*[a]

An original ONP iminophosphorane ligand was synthesised and coordinated to [NiX_2(DME)] (X=Cl, Br). The corresponding complexes (**2X**, X=Cl, Br) were isolated and characterised among others by multinuclear NMR spectroscopy and X-ray crystallography. The collected data suggest that different geometries coexist in solution at room temperature. **2Cl** proved to be an efficient hydrosilylation catalyst able to perform at a loading of 1 mol % in presence of one equivalent SiH_2Ph_2 and 1 mol % of ^{t}BuOK, the reduction of C=C and C=O bonds in high yield in 1 h for most substrates. Moreover, the selective conversion of C=O bond to silylether linkage was observed for nine enones. Therefore, **2Cl** presents a rather unique catalytic behaviour compared to previously described Ni catalysts. Both experimental and theoretical investigations regarding the mechanism suggest the involvement of a Ni-H complex. The computed mechanism presents a highest-lying transition state at only 19.0 kcal mol^{-1} and shows that the reaction is driven by the favorable thermodynamics.

Introduction

Nitrogen-based ligands encompass a large diversity of structures in which the coordinating nitrogen atom can either be sp^3- (amines, amides), sp^2- (imines or N-heterocycles), or sp-hybridised (cyanide). They have found applications in various areas from medicinal chemistry to materials science.[1] In this large variety, iminophosphoranes or phosphinimines (PR_3NR') represent a rather discrete class of ligands.[2] In such derivatives, the nitrogen atom bears two lone pairs which are stabilised via hyperconjugation by the vicinal electropositive phosphorus atom. As a result, it can be described by two different Lewis structures: the ylene form (Figure 1 left), largely used in the literature, which reflects the strong interaction between P and N atoms, and the ylidic form (Figure 1 right) which highlights the strong electron density at the N atom explaining its σ and π electron donating ability. The latter can be modulated via the nitrogen substituent.[3]

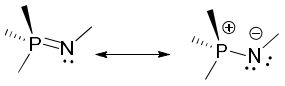

Figure 1: Lewis structures of iminophosphoranes

Even if they were first reported more than a century ago,[4] iminophosphoranes remain underexploited in organometallic catalysis.[2b, 3b, 5]

Nevertheless, they may be of particular interest in catalytic reduction processes due to the high hydridic character of the involved M-H species.[6] Thirty years ago, Cavell and co-workers[7] reported catalytic hydrogenation of olefins with Rh^I complexes supported by mixed phosphine-iminophosphorane ligands. Rh^I or Ir^I catalysts involving other iminophosphorane-based ligands and even chiral ones have been described for this reaction.[8] Moreover, ruthenium or rhodium iminophosphorane complexes have been shown to catalyse the transfer hydrogenation of ketones,[9] in which the solvent (an alcohol) serves as an alternative H-donor. However, there are still very few examples of iminophosphorane catalysts involving earth-abundant metals for these reactions. Fe^{II} iminophosphorane complexes were used successfully for transfer hydrogenation of ketones 15 years ago[10] and more recently for catalytic hydrodefluoration[11] or acetophenone hydrosilylation.[12] To the best or our knowledge, the only examples of iminophosphorane earth-abundant metal complexes used for the catalytic hydrosilylation of olefins are a series of NNN cobalt complexes which are moderately active.[13] Surprisingly, there are no example of iminophosphorane Ni catalysts for this transformation while Ni^{II} complexes were established as powerful hydrosilylation catalysts.[14] In addition, the catalytic ability of iminophosphorane nickel(II) complexes was demonstrated in cross-couplings,[15] ethylene dimerisation reactions,[16] or more recently for reductive couplings[3b] (Scheme 1).

[a] *Laboratoire de Chimie Moléculaire (LCM), CNRS, Ecole Polytechnique, Institut Polytechnique de Paris, Route de Saclay, 91120 Palaiseau, France.*
E-mail: audrey.auffrant@polytechnique.edu
[b] *Institut de Chimie Moléculaire et des Matériaux d'Orsay (UMR CNRS 8182), Paris-Saclay University, bâtiment Henri Moissan, 17 avenue des sciences, 91400 Orsay, France*
E-mail: vincent.gandon@universite-paris-saclay.fr
†Supplementary Information available: [details of any supplementary information available should be included here]. See DOI: 10.1039/x0xx00000x

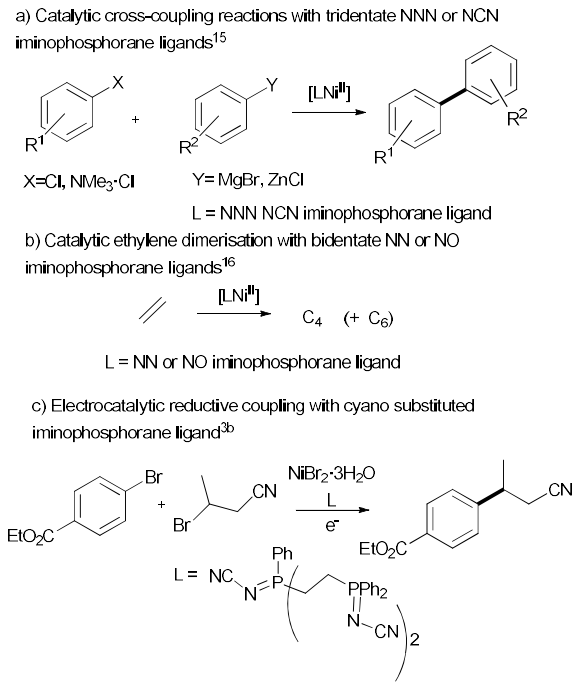

Scheme 1: Catalytic applications of iminophosphorane supported Ni^{II} complexes

This prompted us to investigate whether polydentate iminophosphorane Ni^{II} complexes could serve as hydrosilylation catalysts. We decided to prepare a tridentate L_2X ligand that should afford stable and diamagnetic Ni^{II} complexes. Given our past experience with phosphine-iminophosphorane[16c] and iminophosphorane-phenoxy Ni catalysts,[16d] we focused on a ONP ligand associating these three groups. In this article, we present the synthesis of this original ONP ligand, its coordination to Ni^{II}, as well as the catalytic performance of this ONP Ni complex in the hydrosilylation of olefins, enones, and ketones. DFT calculations regarding the mechanism of the catalytic hydrosilylation are also presented.

Results and discussion

Ligand and Ni complexes synthesis and characterisation

To synthesise the targeted ONP ligand combining a phosphine, an iminophosphorane and a phenoxy group we chose to use the bis(*tert*-butyl)-substituted phenoxyphosphine (Scheme 2), that we previously employed to prepare phosphasalen ligands.[17] The *tert*-butyl groups indeed improved the solubility of the complexes. In order to form the aminophosphonium by the modified Kirsanov procedure we had to synthesise 2-diphenylphosphinoaniline. To do so, we relied on the 3-step-procedure described by Stelzer and coworkers involving the regioselective lithiation of a Boc-protected aniline (Scheme S1),[18] but we had to modify the final deprotection step (see ESI for more information). The aniline obtained after a basic workup is a viscous oil, which proved difficult to precisely weigh, therefore, we chose to isolate it as its ammonium salt. The latter was subsequently engaged in the modified Kirsanov reaction, where the phosphine was first oxidised with one equivalent of bromine in CH_2Cl_2, followed by the addition of one equivalent of DABCO (diazabicycloctane) which was used as a sacrificial base to generate *in situ* the 2-diphenylphosphinoaniline and then trap the equivalent of HBr eliminated while forming the P-NH bond.

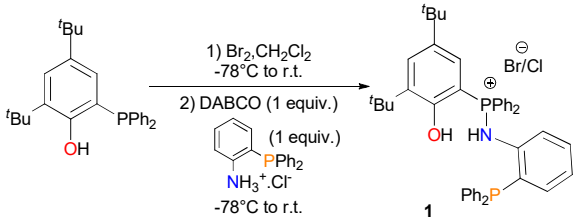

Scheme 2: Synthesis of proligand **1**

The proligand **1** was obtained as a mixture of bromide and chloride salt. Exchanging all the bromide anions for chlorides by stirring with excess chloride salts as well as washing the dichloromethane solution of **1** with saturated aqueous NaCl solution failed to totally exchange the anions. However, as the coordination step with Ni halide salts also produces one salt equivalent, we decided to remove the salt after coordination. The nature of the anions in **1** could be determined by mass-spectrometry and their proportion assessed by X-ray diffraction.

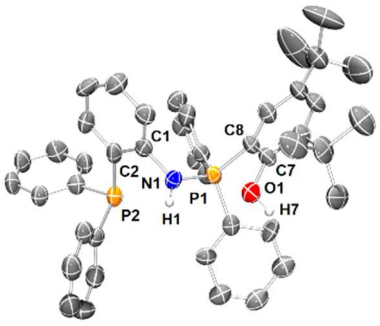

Figure 2: Ortep plot of **1** with thermal ellipsoids (drawn at the 50% probability level). The anion, the H atoms and one $CHCl_3$ molecule have been omitted for clarity. Selected bond lengths [Å] and angles [°]: C7-O1 1.382(4), C8-C7 1.398(5), C8-P1 1.798(4), P1-N1 1.651(3), N1-C1 1.453(4), C1-C2 1.398(5), C2-P2 1.835(4), C1-C2-P2 118.8(3), C2-C1-N1 119.2(3), N1-P1-C8 116.12(16)

The X-ray structure of **1** is shown Figure 2. It presents a zigzag structure. P1 and O1 belong to the plane defined by the phenoxy ring, and N1 and P2 to that of the disubstituted phenyl rings. The angle between these planes is 67.9°. The P1-N1 bond length of 1.651(3) Å is typical of aminophosphonium derivatives.[19] The ^{31}P resonances were observed at -15.6 and 38.0 ppm in $CDCl_3$ for the phosphine and aminophosphonium groups respectively. The ligand was generated *in situ* before coordination (Scheme 3). To the best of our knowledge, this is the first example of an iminophosphorane ONP ligand with a central PN function. The addition of ^{n}BuLi (2 equiv.) to a yellow solution of **1** in THF induced a colour change to orange. The completion of the reaction was ascertained by in situ $^{31}P\{^{1}H\}$ NMR spectroscopy, showing two singlets at 14.6 and -16.5 ppm. After the addition of the nickel precursor either [$NiCl_2$(DME)] or [$NiBr_2$(DME)], the solution darkened. The solvent was evaporated, the residue was washed with pentane and diethyl ether. The obtained red solids were then extracted into toluene to remove the lithium salts and afford complexes **2Cl** and **2Br** in 76% and 68% yield respectively after drying.

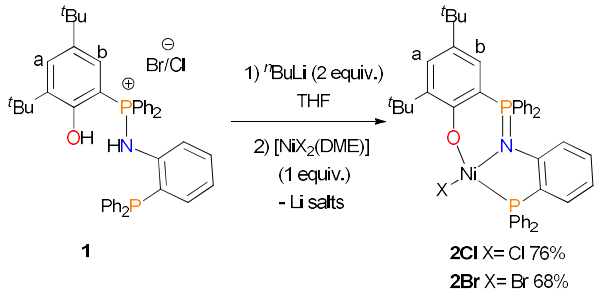

Scheme 3: Synthesis of nickel complexes **2Cl** and **2Br**

These complexes were characterised by multinuclear NMR spectroscopy, X-ray diffraction, and HR-mass spectrometry.

Surprisingly for both complexes, only one ^{31}P resonance was observed at 27 ppm at room temperature while two inequivalent phosphorus nuclei are present in these molecules. To get further information, we recorded VT-NMR spectra in CD_2Cl_2 from -80 to 25 °C. At lower temperature, two resonances were observed at 27.4 and 22.9 ppm for **2Cl**. These values are very close to those reported by Wang and co-workers[20] for a diamagnetic Ni^{II} complex supported by a tridentate NNP L_2X ligand featuring an iminophosphorane, an amide, and a diphenylphosphine (28.7 and 20.0 ppm). This points therefore towards the coordination of both phosphorus groups (as confirmed by X-ray analysis *vide infra*). However, the observed behaviour does not correspond to a classical dynamic phenomenon where two different resonances corresponding to the same nucleus in different environments do change and finally merge upon warming. We did not observe any change in the observed chemical shifts with the temperature, only the appearance of a second peak upon lowering the temperature. We also expanded the window of acquisition (-2000 to 2000 ppm) in order to track a shifted paramagnetic resonance at room temperature, but we did not find any. We were interested in determining to which P-group this behaviour corresponds to and attempted to assign the ^{31}P resonances. A $^{31}P/^{1}H$ 2D experiment was performed: the ^{31}P resonance seen at room temperature correlated with one proton of the N-substituted phenyl and not with those of the phenoxy ring. This has allowed assigning this resonance to the P^{III} nucleus and the shielded one to the iminophosphorane (Figures S8 and S13).‡ The coexistence of different geometries of these complexes in solution, among which some could correspond to paramagnetic compounds, may be an explanation for the behaviour observed. Indeed, the magnetic moment for **2Cl** and **2Br** were measured in solution thanks to the Evans method.[21] Values of 1.52 and 1.12 μ_B for **2Cl** and **2Br**, respectively were obtained at room temperature. They are not unprecedented for tetracoordinatinated Ni^{II} complexes[22] and suggest the coexistence of distorted tetrahedral and square planar geometries in solution at room temperature, with the former hindering the observation of the P^{V} resonance. Given the square planar geometry observed in the solid state (*vide infra*), it would be reasonable to propose that the temperature influences the geometry of the complex, the square planar geometry being dominant at low temperature and the tetrahedral one at higher temperatures. If so, the paramagnetic character would increase upon heating inducing the loss of ^{31}P resonances and the increase of the magnetic moment. This assumption was tested with **2Cl**. Its ^{31}P NMR spectrum was recorded at temperatures in between 25 and 60 °C in $CDCl_3$ (Figure S7) and the disappearance of the ^{31}P resonance was observed around 50 °C. Cooling back to room temperature restored the initial spectrum suggesting the phenomenon is reversible. Moreover, the magnetic moment of **2Cl** measured at -80 °C is almost null, while it reaches 2.89 μ_B at 50 °C. These data agree with a change of the geometry of the complex with the temperature. At low temperature it is square planar (as in the solid state *vide infra*) and acquires a more pronounced tetrahedral character at temperatures above 50 °C. This is reminiscent of the paramagnetic temperature-dependent behaviour of tetraphosphineferrocenyl nickel complexes reported by Hierso and coworkers for which the phosphine resonance was only observed at low temperature.[23] This was also explained by a change in the geometry of the metal.

Single crystals could be grown for both **2Cl** and **2Br**. The structure obtained for **2Cl** is shown in Figure 3. The structure of **2Br**, which was of lower quality, is presented in Figure S1. Both structures are very similar with the Ni in a square planar geometry. In **2Cl**, the nickel atom is distant of 0.017 Å from the plane defined by Cl1, O1, N1. The PN bond measures 1.634(7) Å, which is slightly longer than that reported for the previously mentioned square planar NNP supported nickel chloride complex (1.591(4) Å).[20] Other coordination bond lengths (Ni-Cl, Ni-N, Ni-P) are very similar to those in the latter.

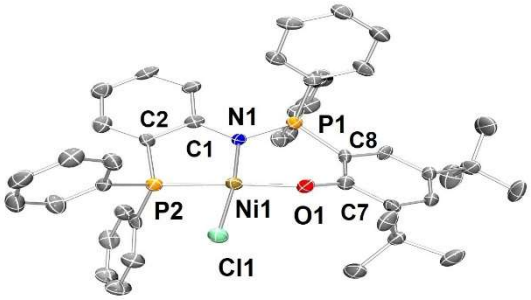

Figure 3: Ortep plot of **2Cl** with thermal ellipsoids (drawn at the 50% probability level). The H atoms and one Et_2O molecule were omitted for clarity. Selected bond lengths [Å] and angles [°]: Ni1-O1 1.876(6), **Ni1-N1 1.935**(8), Ni1-P2 2.114(3), Ni1-Cl1 2.189(3), P1-N1 1.634(7), O1-Ni1-N1 96.8(3), N1-Ni1-P1 87.0(2), P2-Ni1-Cl1 86.12(10), O1-Ni1-Cl1 90.03(19).

Catalysis

Nickel complexes are commonly employed to catalyse the hydrosilylation of alkenes; nevertheless examples of iminophosphorane-supported catalysts for this reaction are limited to a poorly active cobalt catalyst family.[13] With the idea that the reactivity of the M-H active species may be boosted by the electron-donating ability of the iminophosphorane, we evaluated the catalytic behaviour of **2Cl** for the hydrosilylation of 1-octene (Table 1). The reaction was first conducted in diethyl ether at room temperature with one equivalent of diphenylsilane. The conversion and yield were determined by ^{1}H NMR spectroscopy using trimethoxybenzene as an internal reference. Almost no conversion was observed with 1 mol % catalyst (entry 1), but the use of ^{t}BuOK (1 mol %) as an additive

had a very positive impact (entry 2). The linear silane formed exclusively in 97% NMR yield. We confirmed that no reaction occurred in the absence of a nickel complex, while under the same conditions, [$NiCl_2$(DME)] led to 6% conversion only (entries 3 and 4), underlying the importance of the ligand. When **2Br** was used in place of **2Cl** the reaction was slightly less efficient (91% conversion, entry 5). Therefore, we continued the optimisation with **2Cl** as catalyst and tried to decrease the quantity used, nevertheless conversion and yield decreased with the catalytic amount (entries 6-8). Thus, a 1 mol % catalyst loading was used for the rest of the study. We also evaluated other silicon derivatives and employed triethylsilane, and the cheaper triethoxysilane and polymethylhydrosiloxane (PMHS) (Table 1, entries 9-11). The conversion was a little lower and the NMR analysis was not as convenient, therefore we continued with diphenylsilane. We also tested sodium methoxide and a hydride donor ($KHBEt_3$) as additives. The former led to low conversion and yield while the latter gave comparable results (entries 12 and 13). We decided to continue to use ^{t}BuOK and changed the solvent and the concentration. Generally, a lower concentration decreases the efficiency of the reaction (Entry 14 *vs* 2 and 15 *vs* 16). Moreover, substituting diethyl ether by acetonitrile was detrimental to the conversion while changing for THF gave excellent results both at 2 M and 1 M concentration. It therefore offers an alternative in particular when higher temperature may be required for the reaction. Therefore, the conditions of entry 2 which with low additive and catalyst loadings led to an excellent yield in only 1 h were further used to examine the scope of the reaction (Scheme 4).

Table 1: Optimisation of the hydrosilylation of 1-octene[a]

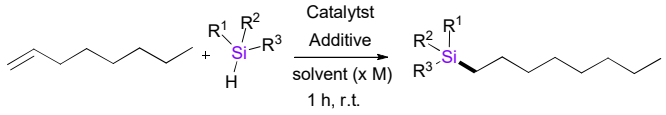

	Catalyst (1 mol %)	Si-H	Solv. (x M)	Additive (1 mol %)	Conv (%)[b]	Yield (%)[c]
1	**2Cl**	SiH_2Ph_2	Et_2O (2)	/	1	1
2	**2Cl**	**SiH_2Ph_2**	**Et_2O (2)**	**^{t}BuOK**	**100**	**97**
3	/	SiH_2Ph_2	Et_2O (2)	/	0	0
4	[$NiCl_2$(DME)]	SiH_2Ph_2	Et_2O (2)	^{t}BuOK	6	6
5	**2Br**	SiH_2Ph_2	Et_2O (2)	^{t}BuOK	91	91
6	**2Cl**[d]	SiH_2Ph_2	Et_2O (2)	^{t}BuOK[d]	66	63
7	**2Cl**[e]	SiH_2Ph_2	Et_2O (2)	^{t}BuOK[e]	45	44
8	**2Cl**[f]	SiH_2Ph_2	Et_2O (2)	^{t}BuOK[f]	17	16
9	**2Cl**	Et_3SiH	Et_2O (2)	^{t}BuOK	79	[g]
10	**2Cl**	$HSi(OEt)_3$	Et_2O (2)	^{t}BuOK	88	[g]
11	**2Cl**	PMHS	Et_2O (2)	^{t}BuOK	100	[g]
12	**2Cl**	SiH_2Ph_2	Et_2O (2)	NaOMe	45	20
13	**2Cl**	SiH_2Ph_2	Et_2O (2)	$KHBEt_3$	97	97
14	**2Cl**	SiH_2Ph_2	Et_2O (1)	^{t}BuOK	94	94
15	**2Cl**	SiH_2Ph_2	MeCN (1)	^{t}BuOK	72	69
16	**2Cl**	SiH_2Ph_2	MeCN (2)	^{t}BuOK	83	83
17	**2Cl**	SiH_2Ph_2	THF (1)	^{t}BuOK	99	98
18	**2Cl**	SiH_2Ph_2	THF (2)	^{t}BuOK	99	99

[a] Reactions were conducted with 1-octene (1 mmol), SiH_2Ph_2 (1 mmol) in diethyl ether at room temperature with 1 mol % catalyst and 1 mol% additive.[b] determined by NMR using the integration of the singlet at 4.92 ppm for SiH_2Ph_2 relative to the CH aromatic resonances of the reference at 6.10 ppm; [c] Determined by NMR using the triplet resonance at 4.86 ppm ($C_8H_{15}SiHPh_2$);[d] 0.8 mol %; [e] 0.5 mol %; [f] 0.2 mol %; [g] Yield could not be determined because of signals overlap from the reagent and the product.

Different aliphatic terminal olefins formed the linear silane (**4a-c**) with high efficiency after 1h. In case of modest yields at room temperature (method A, Scheme S2), a large improvement was observed when heating at 60 °C for 1 h using THF as the solvent (method B). Heteroatoms are relatively well tolerated, as alkylsilanes **4d-f** were obtained in average to high yield. Olefins incorporating a cyclohexene or a phenyl group were efficiently transformed but again some required heating (**3g-3l**). Of note, electron poor or electron rich groups were equally well tolerated (**4k** and **4l**). On the contrary, for styrene derivatives (**3m-3q**) the efficiency and the selectivity of the reaction depends on the nature of the substituent on the aromatic ring. The yield is high from **3m** and **3n**, leading mainly to the linear isomer. From **3o** bearing a more electron-donating methoxy substituent the yield remains high (94%) but both isomers were formed in similar proportions. From **3p** with a chloro substituent, the change in regioselectivity is amplified with the branched isomer **4p'** being twice more present than **4p**. In presence of a more electron-withdrawing group (**3q**) the yield drops but the branched isomer **4q'** becomes largely dominant. The obtention of mixtures of regioisomers from styrene derivatives is not unprecedented in Ni-catalysed hydrosilylation, the preference for the linear[24] or branched[25] product depends on the catalyst. In reports describing the transformation of variously substituted styrenes[25c, 25d, 26] no such change in the regioselectivity was observed with the substituent. Note that α-olefins incorporating a hydroxy group or an aromatic allyl ether were not converted into the silylether. For some of them, competitive experiments showed that they inhibited the catalysis (Schemes S3, S4). We then turned our attention to disubstituted olefins. They were in general poorly reactive even under forcing conditions (Scheme S3). However, 2-octene was converted in **4a** in an excellent 91% yield when using 5 mol % catalyst within one day at 60 °C. In the same conditions α-methylstyrene led to **4r** in 93% NMR yield while **4s** could be isolated in 36% yield.

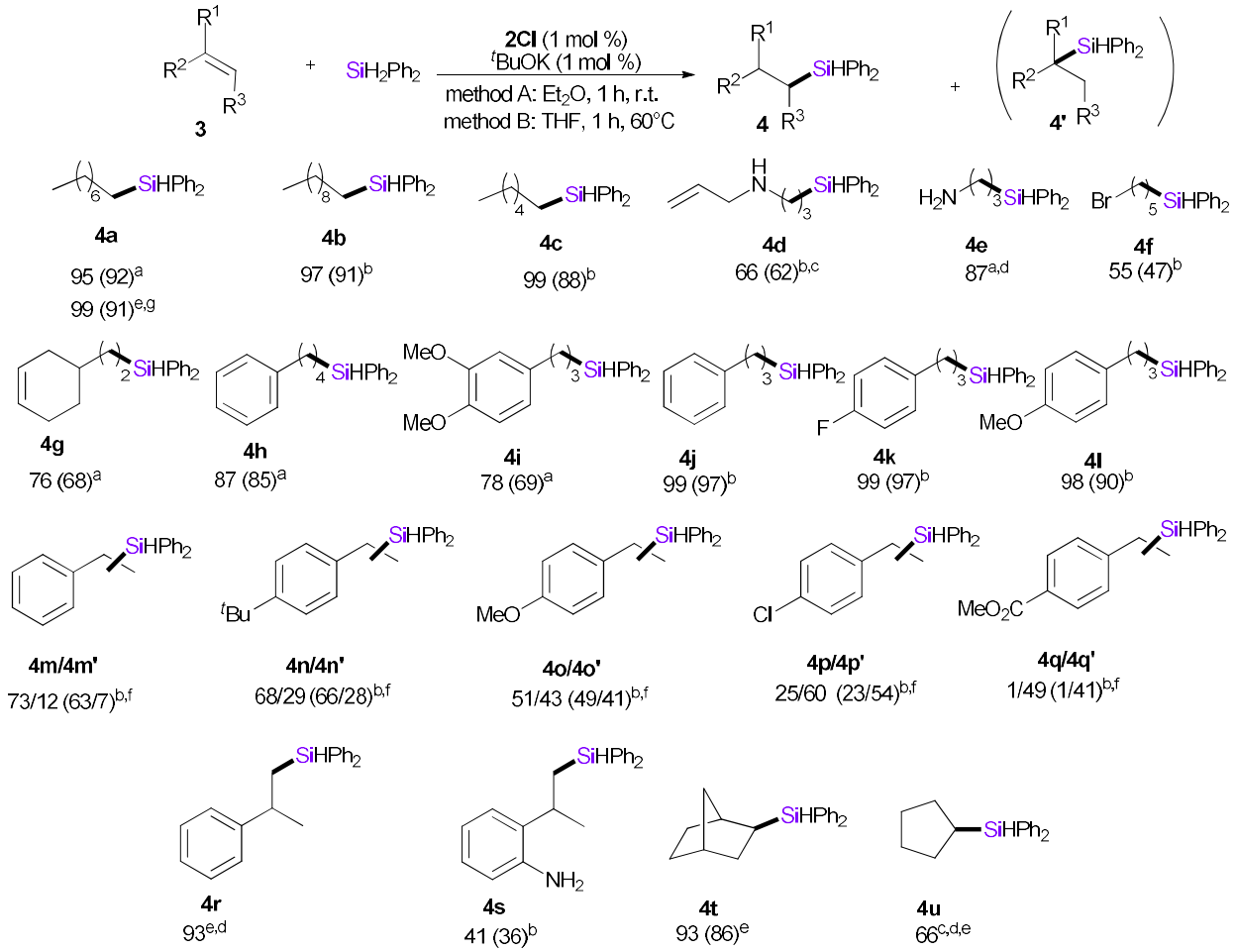

Scheme 4: Scope of the catalytic hydrosilylation of olefins with **2Cl**. NMR yield using trimethoxybenzene as internal reference is given with the isolated yield specified into brackets. [a] Reaction conducted with the olefin (1 mmol) in presence of **2Cl** (0.01 mmol, 1 mol %), trimethoxybenzene (0.07 mmol) as reference, SiH_2Ph_2 (1 mmol), and ^{t}BuOK (0.01 mmol, 1 mol %) for 1 h at room temperature in Et_2O (2M) (Method A). [b] Same conditions as method A but at 60 °C in THF (2M) (Method B). [c] Reaction time extended to 48 h. [d] The product could not be isolated. [e] Reaction conducted for 24 h at 60 °C in THF with 5 mol % of **2Cl** [f] NMR and isolated yield correspond to the mixture of linear and branched product (l/b). [g] Reaction conducted from 2-octene

Moreover, strained internal olefins **3t** and **3u** led to good yields using forcing conditions (60 °C with 5 mol % catalyst for respectively 24 and 48 h). **2Cl** was efficient to catalyse the hydrosilylation of a large range of olefins. In the literature, Ni hydrosilylation catalysts for olefin substrates are reported more often than for carbonyl ones.[14b, 14c] In addition, Hu and coworkers demonstrated the selective conversion of the C=C double bond within keto- and formyl-containing olefins.[27] This stimulated the investigation of the catalytic behaviour of complex **2Cl** with such substrates (Scheme 5).

Surprisingly, **2Cl** catalysed the selective hydrosilylation of the keto group without touching the C=C bond. 4-Hexen-3-one (**5a**), when reacted under the previously described conditions (1 equivalent of diphenylsilane, 1 mol % of **2Cl** as catalyst and ^{t}BuOK as additive in diethyl ether at room temperature), fully converted within 1 h to the vinylsilylether **6'a**, isolated in 93% yield after column chromatography. The latter could result from the hydrosilylation of the C=O followed by an isomerisation of the double bond or from a 1,4 addition. Similarly, **6'b** was isolated in 87% yield when reacting 2-cyclohexen-1-one (**5b**). However, benzylideneacetone (**5c**) was converted to **6c**, in which the position of the double bond had not changed. **6c** was formed with a modest conversion in diethyl ether at room temperature (42%) within 1 h (Scheme S5), while the conversion doubled in THF at 60 °C. This result contrasts with the report from Sortais and Ritleng,[28] showing that the same substrate led to a mixture of compounds resulting from C=O reduction and simultaneous C=O and C=C reduction upon catalysing the hydrosilylation reaction with a N-heterocyclic carbene (NHC) supported nickel complex. The formation of mixtures of compounds was also reported by Rodriguez when reacting enones.[29] However, it remains unclear why the reaction from **5c** occurred without a change of the double bond location. As stated, the reaction temperature influences only the efficiency of the transformation, not the nature of the formed product. Also, 5-hexen-2-one **5d** reacted at room temperature, and *trans*-2-hexenal (**5e**) at 60 °C, both without any change in the double bond position. This phenomenon has been only observed for α,β unsaturated ketones **5a** and **5b**. The hypothesis of a 1,4 hydrosilylation may be contradicted by the inertness of cyclohexene (Scheme S3) under the same reaction conditions. However, the presence of the keto group β to the C=C bond in **5b** may polarise it and favour the reaction. To test

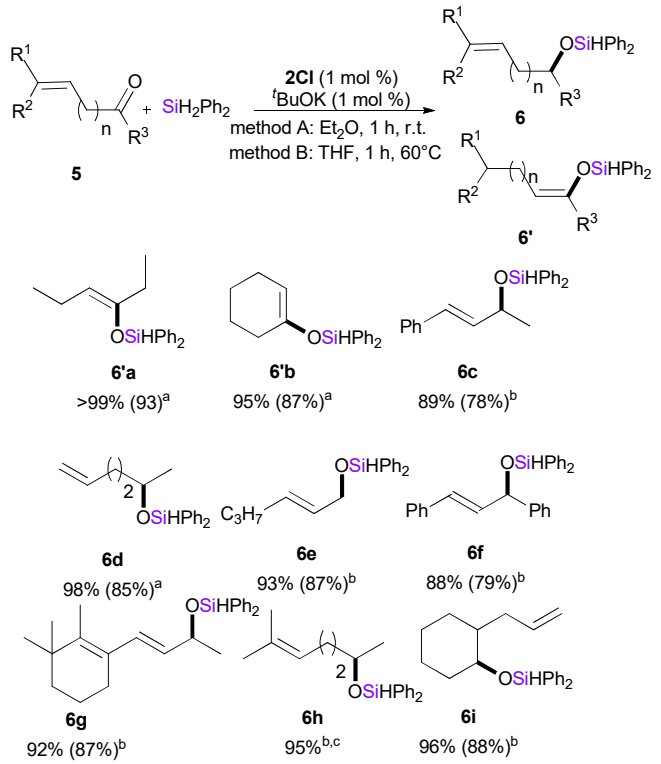

Scheme 5: Scope of the catalytic hydrosilylation of enones/enal with **2Cl**. NMR yield using trimethoxybenzene as internal reference is given with the isolated yield specified into brackets. [a] Reaction conducted with the keto-olefin (1 mmol) in presence of **2Cl** (0.01 mmol, 1 mol %), trimethoxybenzene (0.07 mmol) as reference, SiH_2Ph_2 (1 mmol), and ^tBuOK (0.01 mmol, 1 mol %) within 1 h at room temperature in Et_2O (2 M) (Method A).[b] Same conditions but within 1 h at 60 °C in THF (2 M) (Method B). [b] no isolated yield could be determined

this hypothesis, the hydrosilylation of crotonaldehyde was carried out at room temperature. A full conversion was observed, but a mixture of compounds was obtained as witnessed by ^1H NMR spectroscopy (Figure S16). Indeed, two doublet resonances corresponding to aldehyde protons were identified. These products could result from a non-regioselective double bond hydrosilylation. A 1,4 hydrosilylation would lead to an ethyl substituted vinylether for which a triplet and a quadruplet should be observed. A triplet may be seen at 0.93 ppm ($J_{H,H}$ = 7.5 Hz) but it is superimposed with other resonances and the corresponding quadruplet could not be found. This experiment showed that the reaction outcome from α,β unsaturated ketones highly depends on the substrate structure. Because C=C bond hydrosilylation was observed on crotonaldehyde, we hypothesised that **6'a** and **6'b** result from a 1,4 hydrosilylation. At 60 °C in THF, enones **5f** and **5g** led to the corresponding silylethers which were isolated in high yield. Again, no modification of the double bond was observed, which may be explained by the larger steric hindrance at the γ carbon precluding a 1,4 functionalisation. Therefore, the selectivity of the reaction may arise from a subtle balance between electronic and steric effects in the α,β unsaturated carbonyls tested. Unconjugated ketones **5h-5i** were also efficiently and selectively transformed into the corresponding olefinic silylether **6h-i**.

To the best of our knowledge, **2Cl** represents an unique example of a nickel-based catalyst realising selectively and in high yield the hydrosilylation of a C=O bond in presence of a C=C bond. It nicely complements the pincer nickel complex reported by Hu.[27] Surprisingly, when attempting to convert both the C=C and C=O groups by doubling the amount of silane used, no further conversion of **6d** was observed. Nevertheless, the catalyst remains active since adding one equivalent of silane and one equivalent of 1-octene to the reaction mixture containing **6d** led to an efficient conversion of the latter (Scheme S6).

The catalytic ability of **2c** towards carbonyl substrates was further investigated. We tested the previously established conditions for the hydrosilylation of ketones and were pleased to observe an efficient conversion of a variety of substrates (Scheme 6). Generally, the corresponding alcohol was isolated after methanolysis. As for the olefin and enone substrates, the reaction was first attempted at room temperature for 1 h (method A), and in case of moderate conversion, it was performed in THF for 1 h at 60 °C (method B). Acetophenone and most *para* substituted acetophenones (**7b,c,f**) reacted at room temperature while *p*-cyanoacetophenone **7g** required heating for high conversion (37% at room temperature see Scheme S7). This may be due to detrimental interactions of the CN group with the metal. Electron-donor or -withdrawing groups are equally well tolerated (**8c** vs **8f**), but the position of the substituent impacted the yield (**8c,d,e**). The conversion of o-methoxyacetophenone was lower at 25 °C (24%, Scheme S7) compared to the other isomers, showing the influence of the steric hindrance or of the coordinating ability of the vicinal O atom. Substrates exhibiting larger alkyl substituents on the keto group were also nicely converted at 60 °C, with isolated yield above 85% (**8h-i**). **8j** bearing a long alkyl chain was efficiently formed at room temperature. 3-Methyl-1-phenyl-2-butanone (**7k**), exhibiting a methylene group in between the phenyl and the keto groups, was less reactive than **7h**, giving 71% yield after 14 h at 60 °C. High yields were also obtained starting from benzophenone (**7l**) and heterocyclic substrates (**7m-o**). The thiophene derivative could be easily transformed at room temperature contrary to the pyridine and furan compounds which required heating (prolongated to 2 h in the case of **7o**). Moreover, cyclohexanone and 4-heptanone were efficiently transformed into the corresponding silylethers **8'p** and **8'q**, which were formed in high yield. Of note, Mindiola and coworkers reported a lower yield for **8'p** (70%) when using a nickel pincer dimer (at 2 mol %) after 2.5 h in benzene at 100 °C.[30] A range of aldehydes was also efficiently hydrosilylated. After methanolysis, benzyl alcohols **8r-u** were obtained in high yields. Nevertheless, the reaction time depends on the substituent, **8r** and **8s** being obtained within 1 h while 4 h were necessary to obtain **8u** in high yield. Aliphatic aldehydes were also efficiently converted into the corresponding silylether **8'v-8'x**.

The performance of **2Cl** for the hydrosilylation of aldehydes are comparable to previous Ni catalysts,[14b, 14c] while some reports of efficient aldehyde hydrosilylation at room temperature exist.[31] But for ketones, examples of powerful catalysts under mild conditions remain rare.[14b, 14c] Guan reported only partial hydrosilylation of ketones at 70 °C for 24 h.[31a] Royo on the other hand, described the conversion of acetophenones within some

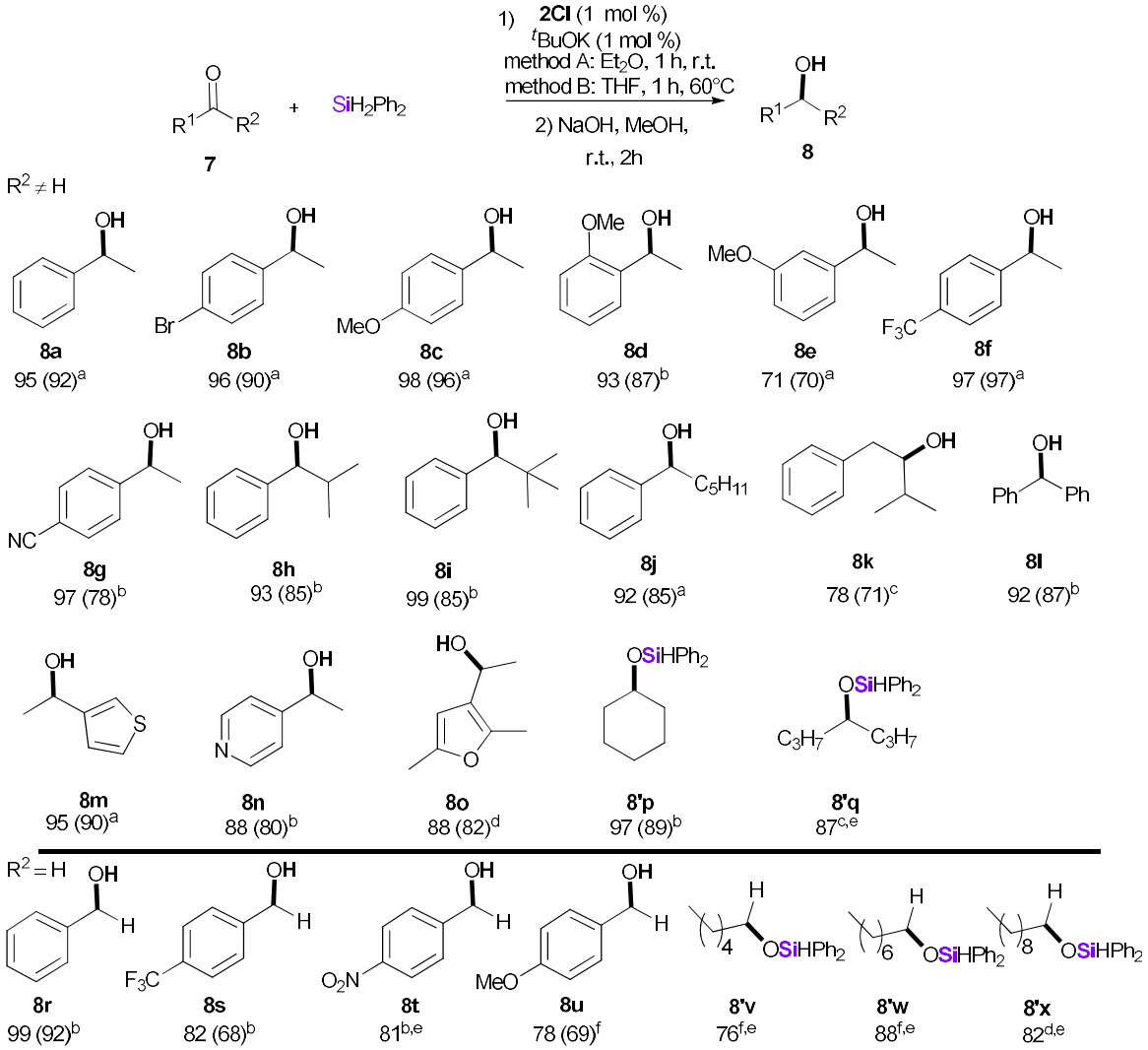

Scheme 6: Scope of the catalytic hydrosilylation of carbonyl compounds with **2Cl**. NMR yield using trimethoxybenzene as internal reference (except for **8v-x** for which trimethylbenzene was employed) is given with the isolated yield specified into brackets. [a] Reaction conducted with the keto-olefin (1 mmol) in presence of **2Cl** (0.0 mmol, 1 mol %), trimethoxybenzene (0.07 mmol) as reference, SiH_2Ph_2 (1 mmol), and ^tBuOK (0.01 mmol, 1 mol %) within 1 h at room temperature in Et_2O (2 M) (Method A). [b] Same conditions but 1 h in THF at 60 °C.[c] Same conditions but 14 h in THF at 60 °C.[d] Same conditions but 2 h in THF at 60 °C.[e] no isolated yield could be determined. [f]Same conditions but 4 h in THF at 60 °C

hours in toluene at 100 °C, while aliphatic derivatives required one day heating.[32] With a similar NHC Ni catalyst, Sortais and Ritleng isolated the corresponding alcohol in good yields after 17 h reaction at 25 °C and methanolysis.[28] More recently, lower performances were reported for comparable substrates with pincer nickel complexes at 70 °C.[29, 33] The catalytic results with **2Cl** for the hydrosilylation of carbonyls are among the best described for a nickel catalyst in the literature. Only the NHC supported Ni complex reported by Ritleng and Sortais gave yields above 70%, on a comparable range of ketones using 5 mol % catalyst within 17 h at room temperature.[28] Noteworthy, competitive hydrosilylation of 1-octene and acetophenone in the established catalytic conditions led to the formation of phenoxydiphenylsilane and octyldiphenylsilane in respectively 98% and 2% yield (Figure S17). This underlines again the preference for C=O over C=C reaction for **2Cl**.

In order to test the robustness of the catalyst regarding scaling-up, as representative examples, the hydrosilylation of 1-octene and acetophenone were performed on the gram scale (Scheme 7). The reactions were conducted neat with 0.1 mol % of **2Cl** and ^tBuOK. Excellent yields were obtained in both cases, but the reaction was much quicker from acetophenone with a total conversion within few minutes (TOF 11 040 h^{-1}). This again demonstrates that **2Cl** is particularly powerful towards ketones.

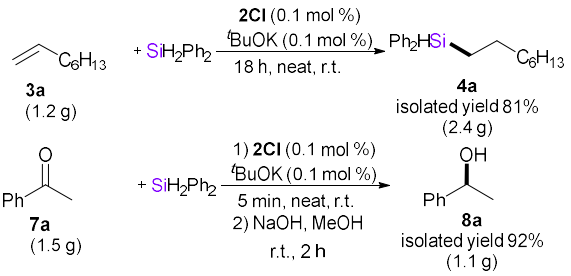

Scheme 7: Gram-scale hydrosilylation of 1-octene and acetophenone

Mechanistic investigations

Given the catalytic performance of **2Cl** for the hydrosilylation of olefins and C=O bonds, we were interested in investigating the mechanism of the reaction. First, when the hydrosilylation of 1-octene was conducted in presence of mercury, the expected silane was obtained in 81% yield (Figure S18) which suggests a homogenous catalytic process. When the reaction was carried out with SiD_2Ph_2 the deuterium atoms were localised in the formed silane on the silicon and the β carbon as expected (Figures S19-21). As such reactions generally involve Ni-H complexes as the active species, the synthesis of **2H** was attempted (Scheme 8-1). However, no compound could be isolated from the reaction of **2Cl** with $KHBEt_3$ (1 equivalent), nevertheless the *in situ* ^1H NMR analysis of the reaction mixture showed a doublet at -25.0 ppm ($J_{P,H}$ = 133.0 ppm) (Figure S22). The latter became a singlet upon phosphorus decoupling. No signal was observed by ^{31}P NMR.

This chemical shift is in the range of Ni-H resonances.[34] The P,H coupling constant is rather large[35] but close to those reported for square planar [(N,P)NNiH] complexes featuring a phosphinoamidinate and a pyridine type ligand.[36] This suggests the formation of a Ni-H complex in which the hydride couples with the PPh_2 group.

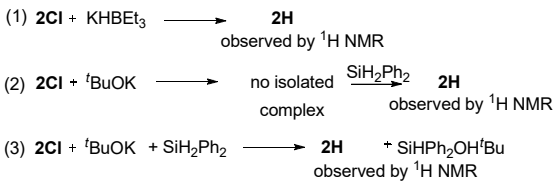

Scheme 8: Attempts to generate reaction intermediates

The synthesis and isolation of **[LNi(O^{t}Bu)]** (**2(O^{t}Bu)**) by addition of ^{t}BuOK to **2Cl** remained unsuccessful. The NMR spectroscopy monitoring provided little information; the ^{31}P resonance was lost suggesting the formation of a paramagnetic species, and the ^1H NMR spectrum was difficult to interpret (Figure S23). But the addition of silane to this mixture led within minutes to a ^1H NMR spectrum very similar to that obtained upon addition of the hydride donor (Scheme 8-(2), Figure S23). Moreover, upon mixing **2Cl** with the silane and ^{t}BuOK in stoichiometric amount in THF at room temperature (Scheme 8-3), a singlet at 5.75 ppm corresponding to the silane $SiHPh_2O^tBu$[37] was observed in the ^1H NMR spectrum as well as the hydride resonance at -25.0 ppm (doublet, $J_{P,H}$ = 133.0 ppm) previously mentioned (Figures S24-25). This reaction was conducted in presence of trimethoxybenzene as reference to quantify the efficiency of the conversion of **2Cl** into **2H**. As shown in Figure S27, the conversion was almost quantitative (96%). In line with the absence of catalytic activity in the absence of additive, no change was observed by NMR upon mixing **2Cl** and the silane. These observations confirm that the Ni-H can form from the alkoxide complex, as previously shown by Hu and coworkers,[27] probably thanks to the silane via σ-bond metathesis[38] (Scheme 9a). Nevertheless, activation of the silane by alkoxides was also described.[39] It was therefore also investigated by ^1H NMR spectroscopy (Scheme 9b and Figure S26). The ^1H NMR spectrum drastically changed upon addition of ^{t}BuOK to SiH_2Ph_2: the initial silane disappears and various species form. Addition to this mixture of **2Cl** led to the observation of the signal characteristic of the Ni-H complex (Figure S26). Therefore, this complex can form by either route depicted in Scheme 9.

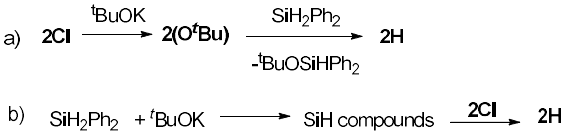

Scheme 9: Possible pathways to form **2H** from **2Cl** under the reaction conditions

As variable temperature NMR studies suggest that the geometry of the precatalyst **2Cl** evolves with the temperature (*vide supra*), the hydrosilylation of 1-octene was attempted at 193K (see Supplementary Information for details). At this temperature, almost no conversion was observed (8%). Although the reaction rate is known to increase with the temperature, the geometry of **2Cl** at low temperature may also disfavour the catalysis.

DFT Calculations

To get a deeper insight into the reaction mechanism, DFT computations were performed using the Gaussian 16[40] set of programs (See computational details). The values presented are ΔG_{298} in kcal mol^{-1}. The putative nickel hydride complex **A**, propene and trimethylsilane were used as model catalyst and substrates (Figure 4). Note that the reaction works with Et_3SiH in a similar manner as with SiH_2Ph_2 (Table 1, entry 9) justifying the simplified model employed. The overall reaction, i.e. the anti-Markovnikov hydrosilylation of propene, is exergonic by 13.5 kcal mol^{-1}. The coordination of propene to Ni can take place without strict ligand exchange, although the Ni–P bond becomes very long (from 2.10 to 3.0 Å). While **A** is virtually square planar, the ONP ligand adopts a butterfly geometry, allowing the 5-coordinate geometry of **B** (8.2 kcal mol^{-1}). Of note involvement of pentacoordinated Ni complexes is not unprecedented in hydrosilylation reactions.[33] However, the low energy level of this intermediate may be surprising considering the structure of the employed ONP ligand. Insertion of propene into the Ni–H bond might lead to the Markovnikov complex **C** or the anti-Markovnikov one **D**. The latter is the only one that can account for the major products observed; however, $\mathbf{TS_{BD}}$ (12.9 kcal mol^{-1}) is 1.0 kcal mol^{-1}less stable than $\mathbf{TS_{BC}}$ (11.9 kcal mol^{-1}). It turns out that the regioselectivity is dependent on the steric hindrance brought about by the alkene substituent (see lower box in Figure 4). The 0.98 kcal mol^{-1} difference between $\mathbf{TS_{BD}}$ and $\mathbf{TS_{BC}}$ with propene is actually lowered to 0.62 kcal mol^{-1} with butene. Albeit small, the selectivity becomes in favor of the anti-Markovnikov process with pentene (-0.28 kcal mol^{-1}). It still increases with hexene (-0.66 kcal mol^{-1}) and even more with heptene (-0.94 kcal mol^{-1}), which is consistent with the experimental findings. Intermediate **D** (7.2 kcal mol^{-1}) is still a 5-coordinate complex due to the coordination of the β-hydrogen. The hydrogen at Ni can be replaced by that of the silane to give intermediate **E** (16.8 kcal mol^{-1}). Through $\mathbf{TS_{EF}}$ (17.2 kcal mol^{-1}), **E** transforms into the 3-center-2-electron complex **F** in a

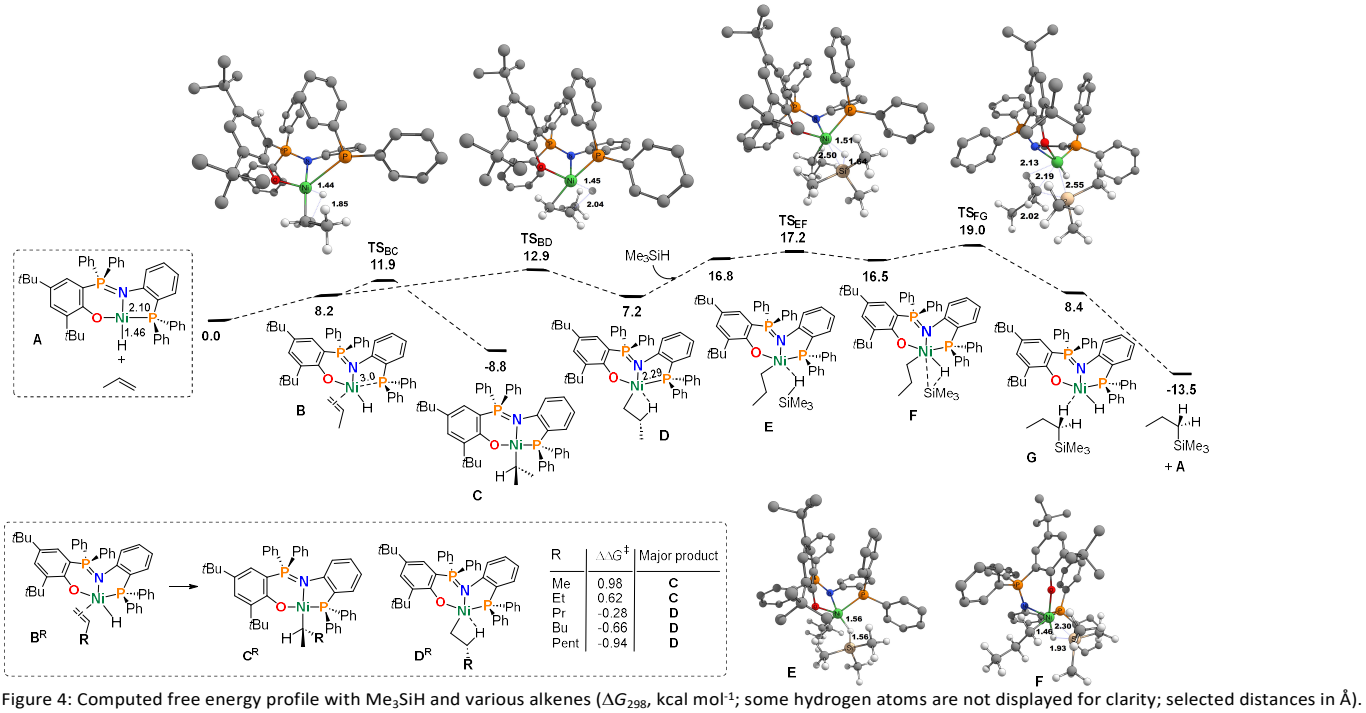

Figure 4: Computed free energy profile with Me_3SiH and various alkenes (ΔG_{298}, kcal mol^{-1}; some hydrogen atoms are not displayed for clarity; selected distances in Å).

virtually thermoneutral manner. This compound can be seen as a Ni^{II} species of the form $[L_2NiX_3]^-$ with a silylium ion ($MeSi^+$) linked to the Ni–H bond. The silylium ion will then play the role of an electrophile in the cleavage of the Ni–C bond via **TS$_{FG}$** (19.0 kcal mol^{-1}) to furnish **G** (8.4 kcal mol^{-1}). As noted above, dissociation of the latter into the hydrosilylation product and **A** is appreciably exergonic. Thus, the highest-lying transition state is located only 19.0 kcal mol^{-1} above the reference system and the driving force of the reaction is the favorable thermodynamics associated to it. This step was reinvestigated with SiH_2Ph_2 and hexene (Figure S130), showing little impact on the overall barrier to reach **TS$_{F'G'}$** (19.7 kcal mol^{-1} vs 19.0 for **TS$_{FG}$**).

Conclusions

An original ONP ligand associating a phenoxide, an iminophosphorane and a phosphine was synthesised from 2-diphenylphosphinoanilinium and a diphenylphosphinophenol derivative. The corresponding Ni^{II} complexes **2X** (X=Cl, Br) were prepared in high yield and characterised by multinuclear NMR spectroscopy, HR-mass spectrometry, elemental analysis and X-ray crystallography. However, the ^{31}P resonance observed at room temperature does not match with the square planar geometry observed in the solid state. Lowering the temperature allows to observe the expected two resonances, but the variable temperature experiments allow to discard a classical hemilability process. For **2Cl**, the NMR experiments and the measurement of magnetic moment at different temperatures suggest the coexistence of square planar and distorted tetrahedral geometries, the former being dominant at low temperature and the latter at temperature around 50 °C. The complexes were tested for the hydrosilylation of olefins. **2Cl** proved particularly efficient, realising the selective conversion into the anti-Markovnikov silylether at 1 mol % loading in presence of 1 mol % of ^{t}BuOK and one equivalent of SiH_2Ph_2 within one hour at room temperature of a variety of olefins, mostly terminal ones. For styrene derivatives, mixture of regioisomers were obtained, the major one depending on the substituent of the aromatic cycle. In some cases, the reaction was conducted at 60 °C, and for some disubstituted olefins longer reaction times or a higher catalyst loading was necessary to obtain good yields. Astoundingly, **2Cl** selectively converted C=O preferentially to C=C in enones, a selectivity that is unprecedented to our knowledge with Ni catalysts. Reduction of carbonyl derivatives (after methanolysis of the vinylether) was also high yielding. In particular a wide range of aromatic and aliphatic ketones was transformed. Therefore, the catalytic results (substrate scope and selectivity) of **2Cl** are rather unique. Mechanism experiments suggest the formation of Ni-H complex (**2H**) under the applied catalytic conditions and the latter was shown by DFT calculations to be able to deliver the hydrosilylation products via a 4-step mechanism. It involves a low-lying pentacoordinated olefin intermediate. The computed mechanism presents a higher activation barrier at 19 kcal mol^{-1} and very favourable thermodynamic parameters. **2Cl** is only the second iminophosphorane earth abundant catalyst to be reported for hydrosilylation reactions. Its excellent performance should stimulate the use of earth-abundant metal catalyst supported by iminophosphorane ligand for reductive transformations. We are currently exploring other catalytic application for this complex and other metal for the coordination of the ligand.

Experimental part

All air and moisture sensitive reactions were performed under inert atmosphere using a vacuum line, inert Schlenk techniques (N_2) and a glove box (Ar, <0.1 ppm H_2O, <0.1 ppm O_2) with oven-dried glassware unless other notified. Reagents were used as received from commercially available suppliers without further purification unless otherwise noticed. CH_2Cl_2, pentane, ether and toluene were taken from solvent purification system (MBraun-SPS). THF was distilled and degassed using freeze-pump technique. NMR spectra were recorded on a Bruker AC-300 SY spectrometer at 300 MHz for ^{1}H, 120 MHz for ^{31}P and 75 MHz for ^{13}C. Solvent peaks were used as internal references for ^{1}H and ^{13}C chemical shifts (ppm). $^{31}P\{^1H\}$ NMR spectra are relative to an 85% H_3PO_4 external reference. Unless otherwise mentioned, NMR spectra were recorded at 300 K. Structural assignments were made with additional information from COSY, HSQC, and HMBC experiments. The spectra were analysed with Topspin software. The following abbreviations are used: s, singlet; d, doublet; dd, doublet of doublets; t, triplet; m, multiplet. The labeling for the proligand and complexes is given in Scheme 3.

Mass spectrometry experiments were performed on a Tims-TOF mass spectrometer (Bruker, France). Electrospray source has been used in positive and negative modes. Samples are prepared in acetonitrile with 0.1 % formic acid at µM concentration. 2 to 10 µL were introduced without separation with Elute UHPLC module (Bruker) at a 100 µL min^{-1} flow rate into the interface of the instrument. Capillary and end plate voltages were set at 4.5 kV and 0.5 kV for ESI experiments. Nitrogen was used as the nebuliser and drying gas at 2 bar and 8 L min^{-1}, respectively, with a drying temperature of 220 °C for ESI source. Tuning mix (Agilent, France) was used for calibration. The elemental compositions of all ions were determined with the instrument software Data Analysis, the precision of mass measurement was less than 3 ppm. Elemental analyses were carried out by the elemental analysis service of the "LCC" (Toulouse) using a PerkinElmer 2400 series II analyser. X-ray crystallography data were collected at 150 K on a Bruker Kappa APEX II diffractometer using a Mo-κ (λ=0.71069Å) X-ray source and a graphite monochromator. The crystal structures were solved using Shelxt[41] or olex[42] and refined using Shelxl-97 or Shelxl-2014.[41] ORTEP drawings were made using ORTEP III[43] for Windows or Mercury. Details of crystal data and structure refinements are summarised in tables S1-2.

Synthesis of 1: Bromide solution in dichloromethane (1.27 mL, 2.47 mmol, 2.0 M) was added dropwise to a cooled (-78°C) solution of 2-diphenylphosphine-4,6-di-*tert*-butylphenol **1** (963.8 mg, 2.47 mmol) in dichloromethane (20 mL). The colorless solution turned yellow and was brought back to room temperature, then stirred for 1 h. Afterwards, the solution was once again cooled to -78°C in order to add DABCO (277.1 mg, 2.47 mmol, 2 equiv.) and 5 min later, a solution of ortho-diphenylphosphine ammonium benzene chloride (932.7 mg, 2.47 mmol) in dichloromethane (6 mL). The yellow solution turned into a brown suspension with a white precipitate, which was warmed to room temperature then stirred for 3 h. Then, the two phases were separated by centrifugation and an excess of potassium chloride (2 g, 27 mmol) was added to the solution. The suspension was stirred for 3h and then the white precipitate was filtered off. The orange solution was concentrated under vacuum to afford a light orange solid. The solid was washed with diethyl ether (10 mL) before being dried under vacuum to give the desired product (**1**), as a light-yellow solid (1.40 g, 2.0 mmol, 81%). Single crystals were grown in $CHCl_3$/pentane layering at room temperature and afforded deep green crystals. $^{31}P\{^1H\}$ NMR ($CDCl_3$, 121.5 MHz, 25 °C): δ -15.6 (s, P^{III}), 38.0 (s, PN); ^{1}H NMR ($CDCl_3$, 300 MHz, 25 °C): δ = 7.62-7.73 (m, 4H, CH_{PPh2}), 7.41-7.52 (m, 8H, CH_{PPh2}), 7.25-7.36 (m, 4H, CH_{PPh2}), 7.06-7.16 (m, 6H, CH_{PPh2} and CH_{Ar}), 7.01 (t, $J_{H,H}$ = 7.5 Hz, 1H, $CH_{Ar\text{-}b}$), 6.79 (m, 1H, CH_{Ar}), 6.73 (m, 1H, CH_{Ar}), 6.71 (m, 1H, $CH_{Ar\text{-}a}$), 1.48 (s, 9H, $(CH_3)_{tBu}$), 1.14 (s, 9H, $(CH_3)_{tBu}$); $^{13}C\{^1H\}$ NMR ($CDCl_3$, 75 MHz, 25 °C) : δ 157.0 (d, $J_{P,C}$ = 3.0 Hz, C_{OH}), 144.6 (d, $J_{P,C}$ = 13.5 Hz, C_{Ar}), 143.5 (d, $J_{P,C}$ = 7.0 Hz, C_{Ar}), 140.8 (d, $J_{P,C}$ = 21.0 Hz, C_{Ar}), 134.9 (d, $J_{P,C}$ = 10.0 Hz, C_{Ar}), 134.3 (s, CH_{PPh2}), 134.2 (d, $J_{P,C}$ = 3.0 Hz, CH_{Ar}), 133.9 (dd, $J_{P,C}$ = 1.5 and 11.5 Hz, CH_{PPh2}), 133.8 (d, $J_{P,C}$ = 20.0 Hz, CH_{PPh2}), 132.0 (s, CH_{PPh2}), 129.9 (s, CH_{Ar}), 129.2 (s, C_{Ar}), 129.0 (d, $J_{P,C}$ = 4.0 Hz, CH_{PPh2}), 128.7 (d, $J_{P,C}$ = 7.0 Hz, CH_{PPh2}), 128.5 (s, CH_{Ar}), 127.9 (d, $J_{P,C}$ = 11.0 Hz, CH_{Ar}), 126.7 (m, CH_{Ar}), 126.4 (s, CH_{Ar}), 121.2 (d, $J_{P,C}$ = 107.0 Hz, C_{PPh2}), 114.7 (d, $J_{P,C}$ = 100.5 Hz, C_{PPh2}), 35.4 (d, $J_{P,C}$ = 1.5 Hz, C_{tBu}), 34.6 (s, C_{tBu}), 31.2 (s, $(CH_3)_{tBu}$), 30.6 (s, $(CH_3)_{tBu}$). HR-MS (ESI$^+$): calculated for $[C_{44}H_{46}NOP_2]^+$ ([M-X]$^+$) 666.3049; found 666.3036.

Synthesis of 2Cl: ^{n}BuLi (0.94 mL of a 1.6 M ether solution, 1.5 mmol,) were added to a cooled (-78°C) solution of **1** (547.5 mg, 0.75 mmol) in tetrahydrofuran (40 mL). The yellow solution turns orange upon warming to room temperature and the deprotonation was completed after 10 min. [$NiCl_2$(DME)] (164.8 mg, 0.75 mmol) was added to the orange solution of the iminophosphorane, the solution turned dark red/maroon and was stirred 30 min. The solvent was evaporated under vacuum and dichloromethane (40 mL) was added. A white precipitate appears and was filtered off on a PTFE filter. The solvent was evaporated under vacuum then the dark red solid was washed with a 1 : 3 Et_2O : pentane mixture (20 mL). The desired complex **2Cl** was extracted into toluene (80 mL). This solvent was evaporated, and **2Cl** was obtained as a dark red solid after drying under vacuum (430.0 mg, 0.58 mmol, 76%). Single crystals were obtained by diffusion of diethyl ether in THF solution. $^{31}P\{^1H\}$ NMR (CD_2Cl_2, 121.5 MHz, -80 °C): δ = 27.4 (s), 23.0 (s); ^{1}H NMR ($CDCl_3$, 300 MHz, 25 °C): δ = 7.93 (m, 4H, CH_{PPh2}), 7.40-7.61 (m, 16H, CH_{PPh2}), 7.37-7.39 (m, 1H, CH_a), 6.96 (d, $J_{H,H}$ = 7.5 Hz, 1H, CH), 6.73 (td, $J_{H,H}$ = 1.5 and 7.5Hz, 1H, CH), 6.53 (t, $J_{H,H}$ = 7.5 Hz, 1H, CH), 6.26 (d, $J_{H,H}$ = 8.5 Hz, 1H, CH), 6.21 (dd, $J_{H,H}$ = 2.5 and $J_{P,H}$ = 7.5 Hz, 1H, CH_b), 1.34 (s, 9H, $(CH_3)_{tBu}$), 1.07 (s, 9H, $(CH_3)_{tBu}$);$^{13}C\{^1H\}$ NMR ($CDCl_3$, 75 MHz, 25 °C): δ= 168.1 (s, C_O), 156.2 (s, C_N), 144.3 (s, C_{Ar}), 134.8 (s, C_{Ar}), 134.2 (s, CH_{PPh2}), 133.0 (d, $J_{P,C}$ = 9.5 Hz, CH_{PPh2}), 132.9 (s, CH), 132.5 (d, $J_{P,C}$ = 3.0 Hz, CH_{PPh2}), 132.1 (d, $J_{P,C}$ = 10.5 Hz, C_{Ar}), 131.5 (s, CH), 130.9 (s, CH_{PPh2}), 129.7 (s, CH_b), 129.6 (d, $J_{P,C}$ = 9.0 Hz, C_{Ar}), 129.0 (d, $J_{P,C}$ = 12.5 Hz, CH_{PPh2}), 128.6 (s, CH_{PPh2}), 127.0 (d, $J_{P,C}$ = 92.0 Hz, C_{PPh2}),125.6 (d, $J_{P,C}$ = 6.5 Hz, CH_a), 121.3 (d, $J_{P,C}$ = 9.5 Hz, CH), 119.5 (s, CH), 114.0 (d, $J_{P,C}$ = 126.0 Hz, C_{PPh2}), 35.3 (s, C_{tBu}), 33.8 (s, C_{tBu}), 31.4 (s, $(CH_3)_{tBu}$), 30.2 (s, $(CH_3)_{tBu}$). HR-MS (ESI$^+$):

calculated for $[C_{44}H_{44}NNiOP_2]^+$ ([M-Cl]$^+$) 722.2246; found 722.2244. Anal. Calcd for $C_{44}H_{44}ClNNiOP_2$.0.5 C_8H_8: C, 70.64; H, 5.98; N, 1.76. Found: C, 70.39; H, 6.43; N, 1.93.

Synthesis of 2Br: It was synthesised as **2Cl** reacting ^{n}BuLi (0.19 mL of a 1.6 M ether solution, 0.3 mmol), **1** (105.7 mg, 0.15 mmol) and [$NiBr_2$(DME)] (46.3 mg, 0.3 mmol) in THF (15 mL). The solid residue was washed with a 1 : 3 Et_2O : pentane mixture (8 mL). **2Br** was obtained as a dark red (80.8 mg, 0.10 mmol, 68%) after extraction into toluene (30 mL) and drying under vacuum. Single crystals were obtained by diffusion of diethyl ether in THF solution. $^{31}P\{^1H\}$ NMR (CD_2Cl_2, 121.5 MHz, -80 °C): δ = 27.3 (s), 22.8 (s); ^1H NMR (CD_2Cl_2, 300 MHz, 25 °C): δ = 7.93 (dd, $J_{H,H}$ = 2.0 and 7.5Hz, 4H, CH_{PPh2}), 7.56-7.67 (m , 16H, CH_{PPh2}), 7.44-7.46 (m , 1H, $CH_{Ar\text{-}b}$), 6.89 (d, $J_{H,H}$ = 7.5 Hz, 1H, CH_{Ar}), 6.78 (t, $J_{H,H}$ = 7.5Hz, 1H, CH_{Ar}), 6.56 (t, $J_{H,H}$ = 7.5 Hz, 1H, CH_{Ar}), 6.28-6.33 (m, 2H, CH_{Ar} and $CH_{Ar\text{-}a}$), 1.32 (s, 9H, (CH_3)$_{tBu}$), 1.10 (s, 9H, (CH_3)$_{tBu}$); $^{13}C\{^1H\}$ NMR ($CDCl_3$, 75 MHz, 25 °C): δ= 167.0 (s, C_O), 157.0 (s, C_N), 144.3 (s, C_{Ar}), 144.1 (s, C_{Ar}), 135.4 (d, $J_{P,C}$ = 14.5 Hz, C_{Ar}), 134.4 (s, CH_{PPh2}), 133.2 (s, CH_{Ar}), 133.1 (d, $J_{P,C}$ = 10.0 Hz, CH_{PPh2}), 131.7 (s, CH_{Ar}), 132.8 (d, $J_{P,C}$ = 3.0 Hz, CH_{PPh2}), 131.0 (s, CH_{PPh2}), 129.6 (s, $CH_{Ar\text{-}b}$), 129.0 (d, $J_{P,C}$ = 12.5 Hz, CH_{PPh2}), 128.6 (s, CH_{PPh2}), 126.9 (d, $J_{P,C}$ = 93.0 Hz, C_{PPh2}), 126.1 (d, $J_{P,C}$ = 7.0 Hz, C_{Ar}), 125.6 (d, $J_{P,C}$ = 14.5 Hz, $CH_{Ar\text{-}a}$), 121.4 (d, $J_{P,C}$ = 7.5 Hz, CH_{Ar}), 119.8 (s, CH_{Ar}), 115.0 (d, $J_{P,C}$ = 111.0 Hz, C_{PPh2}), 35.0 (s, C_{tBu}), 33.6 (s, C_{tBu}), 31.1 (s, (CH_3)$_{tBu}$), 30.0 (s, (CH_3)$_{tBu}$); HR-MS (ESI$^+$): calculated for $[C_{44}H_{44}NNiOP_2]^+$ ([M-Br]$^+$ 722.2246; found 722.2239. Anal. Calcd for $C_{44}H_{44}BrNNiOP_2$.1.5 C_8H_8: C, 69.52; H, 5.99; N, 1.49. Found: C, 69.44; H, 6.32; N, 1.58.

General procedure for the catalytic hydrosilylation of alkenes 3: In the glovebox, trimethoxybenzene (11.8 mg, 0.07 mmol) and **2Cl** (7.6 mg, 0.01 mmol, 1 mol %) were introduced in a 10 mL vial. Then, SiH_2Ph_2 (0,19 mL, 1 mmol, 1 equiv.) and the alkene (1 mmol, 1 equiv.) were added. Finally, the corresponding volume of solvent either Et_2O for the reaction performed at 25 °C (Method A) or THF for these performed at 60 °C (Method B) to reach a 2M concentration and ^{t}BuOK (1.1 mg, 0.01 mmol, 1 mol %) were added and the vial was capped. After stirring 1h at the appropriate temperature, an aliquot of 10µL was taken, quenched with 1 mL of distilled water and extracted with 2.5 mL of Et_2O then dried on $MgSO_4$. The solvent from the aliquot was evaporated on the rotary evaporator (5 min, 50 mbar, 40 °C) and analysed by NMR in $CDCl_3$. The rest of the mixture was put on the rotary evaporator (30 min, 50 mbar, 40 °C) and then the crude product was purified by flash chromatography (pentane/EtOAc) and the desired silyl ether was isolated.

General procedure for the catalytic hydrosilylation of enones/enals 5: In the glovebox, trimethoxybenzene (11.8 mg, 0.07 mmol) then **2Cl** (7.6 mg, 0.01 mmol, 1 mol %) were introduced in a 6 mL catalytic vial. Then, SiH_2Ph_2 (0,19 mL, 1 mmol, 1 equiv.), the enone or enal **5** (1 mmol, 1 equiv.) were also introduced. The corresponding volume of solvent; Et_2O if the reaction would be performed at 25 °C (Method A) or THF if reaction would be performed at 60 °C (Method A), to reach a 2M solution, and ^{t}BuOK (1.1 mg, 0.01 mmol, 1 mol %) were added and the vial was capped. After stirring 1 h at the appropriate temperature, an aliquot of 10 µL was taken, quenched with 1 mL of distilled water and extracted with 2.5 mL of Et2O then dried on $MgSO_4$. The solvent from the aliquot was evaporated on the rotary evaporator (5 min, 50 mbar, 40 °C) and analysed by NMR in $CDCl_3$. The rest of the mixture was put on the rotary evaporator (30 min, 50 mbar, 40 °C) and then the crude product was purified by flash chromatography (pentane/EtOAc) and the desired silyl ether was isolated.

General procedure for the catalytic hydrosilylation of ketones and aldehydes 7: In the glovebox, trimethoxybenzene (11.8 mg, 0.07mmol) then **2Cl** (7.6 mg, 0.01 mmol, 1 mol %) were introduced in a 6 mL catalytic vial. Then, SiH_2Ph_2 (0,19 mL, 1 mmol, 1 equiv.) and the ketone derivative **7** (1 mmol, 1 equiv.) were also introduced. Finally, the corresponding volume of solvent; Et_2O if the reaction would be performed at 25 °C (Method A) or THF if reaction would be performed at 60 °C (Method A), to reach a 2M solution, and ^{t}BuOK (1.1 mg, 0.01 mmol, 1 mol %) were added and the vial was capped. After stirring 1h at the appropriate temperature, an aliquot of 10 µL was taken, quenched with 1 mL of distilled water and extracted with 2.5 mL of Et_2O then dried on $MgSO_4$. The solvent from the aliquot was evaporated on the rotary evaporator (5 min, 50 mbar, 40 °C) and analysed by NMR in $CDCl_3$. The rest of the mixture was reacted with 3 mL of a saturated NaOH solution in MeOH during 2h at room temperature. Then, water (5 mL) and Et_2O (10 mL) were added and the aqueous layer was further extracted with Et_2O (2 x 20mL). The combined organic layers were washed with brine (5 mL) and concentrated under vacuum. Afterwards, the crude product was purified by flash chromatography (pentane/EtOAc) and the desired alcohol **8** was isolated. In the case of **7n** and **7o**, after the aliquot was taken, the rest of the reaction mixture was put on the rotary evaporator (30 min, 50 mbar, 40 °C) and then the crude product was purified by flash chromatography (pentane/EtOAc) and the desired silyl ether was isolated.

Computational Details: Optimisations were carried out with the M06 functional,[44] the LANL2DZ ECP basis set[45] for Ni and the 6-31G(d,p) basis set for the other elements. Thermal correction to the Gibbs free energy was obtained at the optimisation level. Single point energy calculations were performed M06-2X/def2-TZVPP level.[46]

Author contributions

I. P.: formal analysis, data curation, and investigation. T. F. A. A.: investigation. S. B.: formal analysis, data curation. N. C.: formal analysis, data curation. V.G.: formal analysis, data curation. A. A.: formal analysis, data curation, supervision, writing of the original draft.

Conflicts of interest

The authors declare no conflict of interest.

Data availability

The data supporting this article have been included as part of the Supplementary Information.

Acknowledgements

The authors thank Ecole Polytechnique, CNRS, and UPSaclay for financial support and Mr. Karim Hammad for his help in recording the 2D H/P NMR experiments. This work was granted access to the HPC resources of CINES under the allocation 2020-A0070810977 made by GENCI to VG. The Agence Nationale de la Recherche (ANR-21-CE07-0026) is acknowledged for funding the LYMACATO project, and RESOMAG platform for the access to NMR instruments, as well as GDR Phosphore for gathering the community of P-chemist in France.

Notes and references

‡ The same 2D NMR experiment performed at -80 °C was not conclusive because the resolution was not sufficient to confidently assign the cross peak to one or the other of the broad ^{31}P resonances.

1. (a) See articles in this theme issue: A. J. L. Pombeiro, Nitrogen ligands. *Dalton Trans.* 2019**, 48** (37), 13904-13906; (b) L. Kótai, Metal Complexes with N-donor Ligands. *Inorganics* 2024**, 12** (5).
2. (a) S. E. García-Garrido; A. Presa Soto; J. García-Álvarez, Chapter Three - Iminophosphoranes (R3PNR'): From terminal to multidentate ligands in organometallic chemistry. In *Advances in Organometallic Chemistry*, Pérez, P. J., Ed. Academic Press: 2022; Vol. 77, pp 105-168; (b) T. Tannoux; A. Auffrant, Complexes featuring tridentate iminophosphorane ligands: Synthesis, reactivity, and catalysis. *Coord. Chem. Rev.* 2023**, 474**, 214845.
3. (a) I. Popovici; C. Barthes; T. Tannoux; C. Duhayon; N. Casaretto; A. Monari; A. Auffrant; Y. Canac, Phosphonium Ylides vs Iminophosphoranes: The Role of the Coordinating Ylidic Atom in cis-[Phosphine-Ylide $Rh(CO)_2$] Complexes. *Inorg. Chem.* 2023**, 62** (5), 2376-2388; (b) V. Mdluli; D. Lehnherr; Y.-h. Lam; M. T. Chaudhry; J. A. Newman; J. O. DaSilva; E. L. Regalado, Electrosynthesis of iminophosphoranes and applications in nickel catalysis. *Chem. Sci.* 2024**, 15** (16), 5980-5992; (c) I. Popovici; E. Lognon; N. Casaretto; A. Monari; A. Auffrant, Electronic Effects in Phosphino-Iminophosphorane PdII Complexes upon Varying the N Substituent. *Chem. Eur. J.* 2024**, 30** (5), e202303350.
4. H. Staudinger; J. Meyer, Über neue organische Phosphorverbindungen III. Phosphinmethylenderivate und Phosphinimine. *Helv. Chim. Acta* 1919**, 2** (1), 635-646.
5. J. García-Álvarez; S. E. García-Garrido; V. Cadierno, Iminophosphorane–phosphines: Versatile ligands for homogeneous catalysis. *J. Organomet. Chem.* 2014**, 751**, 792-808.
6. M. M. H. Sung; D. E. Prokopchuk; R. H. Morris, Phosphine-free ruthenium NCN-ligand complexes and their use in catalytic CO_2 hydrogenation. *Dalton Trans.* 2019**, 48** (44), 16569-16577.
7. D. J. Law; R. G. Cavell, Homogeneous hydrogenation of olefins catalysed by rhodium(I) complexes of new heterodifunctional phosphorus—nitrogen chelating ligands. *J. Mol. Catal.* 1994**, 91** (2), 175-186.
8. (a) T. T. Co; T.-J. Kim, Chiral (iminophosphoranyl)ferrocenes: highly efficient ligands for rhodium- and iridium-catalyzed enantioselective hydrogenation of unfunctionalized olefins. *Chem. Commun.* 2006**,** (33), 3537-3539; (b) R. Venkateswaran; M. S. Balakrishna; S. M. Mobin, The Iminophosphorane-Phosphane $Ph_2PC_6H_4OC_6H_4PPh_2$=NP(O)$(OPh)_2$: Synthesis, Reactivity, and Catalytic Activity in Suzuki Cross-Coupling and the Homogeneous Hydrogenation of Olefins. *Eur. J. Inorg. Chem.* 2007**, 2007** (13), 1930-1938.
9. (a) V. Cadierno; P. Crochet; J. García-Álvarez; S. E. García-Garrido; J. Gimeno, Neutral and cationic (η6-arene)-ruthenium(II) complexes containing the iminophosphorane–phosphine ligand Ph_2PCH_2P(=N-p-C_5F_4N)Ph_2: influence of the arene ring in catalytic transfer hydrogenation of cyclohexanone. *J. Organomet. Chem.* 2002**, 663** (1), 32-39; (b) V. Cadierno; P. Crochet; J. Díez; J. García-Álvarez; S. E. García-Garrido; S. García-Granda; J. Gimeno; M. A. Rodríguez, Synthesis, reactivity and catalytic activity in transfer hydrogenation of ketones of ruthenium(ii) and ruthenium(iv) complexes containing the novel N-thiophosphorylated iminophosphorane-phosphine ligands Ph_2PCH_2P{=NP(=S)$(OR)_2$}Ph_2 (R = Et, Ph). *Dalton Trans.* 2003**,** (16), 3240-3249; (c) V. Cadierno; P. Crochet; J. Díez; J. García-Álvarez; S. E. García-Garrido; J. Gimeno; S. García-Granda; M. A. Rodríguez, Ruthenium(II) and Ruthenium(IV) Complexes Containing κ^1-P-, κ2-P,O-, and κ^3-P,N,O-Iminophosphorane-Phosphine Ligands Ph_2PCH_2P{NP(O)$(OR)_2$}Ph_2 (R = Et, Ph): Synthesis, Reactivity, Theoretical Studies, and Catalytic Activity in Transfer Hydrogenation of Cyclohexanone. *Inorg. Chem.* 2003**, 42** (10), 3293-3307; (d) A. Buchard; E. Payet; A. Auffrant; X. Le Goff; P. Le Floch, Iminophosphorane-based P_2N_2 rhodium complexes: synthesis, reactivity, and application in catalysed transfer hydrogenation of polar bonds. *New J. Chem.* 2010**, 34** (12), 2943-2949; (e) A. Picot; H. Dyer; A. Buchard; A. Auffrant; L. Vendier; P. Le Floch; S. Sabo-Etienne, Interplay between Hydrido/Dihydrogen and Amine/Amido Ligands in Ruthenium-Catalyzed Transfer Hydrogenation of Ketones. *Inorg. Chem.* 2010**, 49** (4), 1310-1312; (f) H. Dyer; A. Picot; L. Vendier; A. Auffrant; P. Le Floch; S. Sabo-Etienne, Tridentate and Tetradentate Iminophosphorane-Based Ruthenium Complexes in Catalytic Transfer Hydrogenation of Ketones. *Organometallics* 2011**, 30** (6), 1478-1486.
10. A. Buchard; H. Heuclin; A. Auffrant; X. F. Le Goff; P. Le Floch, Coordination of tetradentate X(2)N(2) (X = P, S, O) ligands to iron(II) metal center and catalytic application in the transfer hydrogenation of ketones. *Dalton Trans.* 2009**,** (9), 1659-1667.
11. N. M. Hein; F. S. Pick; M. D. Fryzuk, Synthesis and Reactivity of a Low-Coordinate Iron(II) Hydride Complex: Applications in Catalytic Hydrodefluorination. *Inorg. Chem.* 2017**, 56** (23), 14513-14523.
12. T. Tannoux; L. Mazaud; T. Cheisson; N. Casaretto; A. Auffrant, FeII complexes supported by an iminophosphorane ligand: synthesis and reactivity. *Dalton Trans.* 2023**, 52** (34), 12010-12019.
13. T. Suzuki; H. Masuda; M. D. Fryzuk, Variable coordination geometries via an amine-tethered-enamidophosphinimine ligand on cobalt. *Dalton Trans.* 2017**, 46** (20), 6612-6622.
14. (a) X. Du; Z. Huang, Advances in Base-Metal-Catalyzed Alkene Hydrosilylation. *ACS Catal.* 2017**, 7** (2), 1227-1243; (b) B. Royo, Chapter Two - Recent advances in catalytic hydrosilylation of carbonyl groups mediated by well-defined first-row late transition metals. In *Advances in Organometallic Chemistry*, Pérez, P. J., Ed. Academic Press: 2019; Vol. 72, pp 59-102; (c) V. Arora; H. Narjinari; P. G. Nandi; A. Kumar, Recent advances in pincer–nickel catalyzed reactions. *Dalton Trans.* 2021**, 50** (10), 3394-3428; (d) L. D. de Almeida; H. Wang; K. Junge; X. Cui; M. Beller, Recent Advances in Catalytic Hydrosilylations: Developments beyond Traditional Platinum Catalysts. *Angew. Chem. Int. Ed.* 2021**, 60** (2), 550-565.
15. (a) L. Wang; Z.-X. Wang, Efficient cross-coupling of aryl chlorides with arylzinc reagents catalyzed by amido pincer complexes of nickel. *Org. Lett.* 2007**, 9** (21), 4335-4338; (b) Z.-X. Wang; L. Wang, Amido pincer complex of nickel-catalysed Kumada cross-coupling reactions. *Chem. Commun.* 2007**,** (23), 2423-2425; (c) C. Zhang; Z. X. Wang, N-Heterocyclic Carbene-Based Nickel Complexes: Synthesis and Catalysis in Cross-

Couplings of Aryl Chlorides with ArMX (M = Mg or Zn). *Organometallics* 2009**, 28** (22), 6507-6514; (d) Q. Zhang; X. Q. Zhang; Z. X. Wang, Nickel complexes supported by quinoline-based ligands: synthesis, characterization and catalysis in the cross-coupling of arylzinc reagents and aryl chlorides or aryltrimethylammonium salts. *Dalton Trans.* 2012**, 41** (34), 10453-10464; (e) X. Q. Zhang; Z. X. Wang, Cross-Coupling of Aryltrimethylammonium Iodides with Arylzinc Reagents Catalyzed by Amido Pincer Nickel Complexes. *J. Org. Chem.* 2012**, 77** (7), 3658-3663; (f) W. J. Guo; Z. X. Wang, Cross-Coupling of ArX with ArMgBr Catalyzed by N-Heterocyclic Carbene-Based Nickel Complexes. *J. Org. Chem.* 2013**, 78** (3), 1054-1061.

16. (a) M. Sauthier; F. Leca; R. Fernando de Souza; K. Bernardo-Gusmão; L. F. Trevisan Queiroz; L. Toupet; R. Réau, NiCl2(1,2-Diiminophosphorane) complexes: a new family of readily accessible and tuneable catalysts for oligomerisation of ethylene. *New J. Chem.* 2002**, 26** (5), 630-635; (b) C. Zhang; W.-H. Sun; Z.-X. Wang, Cobalt and nickel complexes bearing pyrazolyliminophosphorane ligands: Synthesis, characterisation and catalytic ethylene oligomerisation behaviour. *Eur. J. Inorg. Chem.* 2006**,** (23), 4895-4902; (c) A. Buchard; A. Auffrant; C. Klemps; L. Vu-Do; L. Boubekeur; X. F. Le Goff; P. Le Floch, Highly efficient P-N nickel(II) complexes for the dimerisation of ethylene. *Chem. Commun.* 2007**,** (15), 1502-1504; (d) T. Cheisson; T.-P.-A. Cao; X. F. Le Goff; A. Auffrant, Nickel Complexes Featuring Iminophosphorane-Phenoxide Ligands for Catalytic Ethylene Dimerization. *Organometallics* 2014**, 33** (21), 6193-6199.

17. (a) C. Bakewell; T. P. A. Cao; N. Long; X. F. Le Goff; A. Auffrant; C. K. Williams, Yttrium Phosphasalen Initiators for rac-Lactide Polymerization: Excellent Rates and High Iso-Selectivities. *J. Am. Chem. Soc.* 2012**, 134** (51), 20577-20580; (b) I. Mustieles-Marín; A. Auffrant, Phosphasalen vs. Salen Ligands: What Does the Phosphorus Change? *Eur. J. Inorg. Chem.* 2018**, 2018** (15), 1634-1644.

18. A. Heßler; K. W. Kottsieper; S. Schenk; M. Tepper; O. Stelzer, A Novel Access to Tertiary and Secondary ortho-Aminophenylphosphines by Protected Group Synthesis and Palladium Catalyzed P-C Coupling Reactions. *Z. Naturrforsch. B* 2001**, 56** (4-5), 347-353.

19. (a) T. Vijayakanth; A. K. Srivastava; F. Ram; P. Kulkarni; K. Shanmuganathan; B. Praveenkumar; R. Boomishankar, A Flexible Composite Mechanical Energy Harvester from a Ferroelectric Organoamino Phosphonium Salt. *Angew. Chem. Int. Ed.* 2018**, 57** (29), 9054-9058; (b) G. Albertin; S. Antoniutti; J. Castro, Reactions of $IrHCl_2(PPh_3)_2\{P(OEt)_3\}$ with Organic Azides: Formation of Aminophosphonium Salts. *Zeitschrift für anorganische und allgemeine Chemie* 2014**, 640** (1), 136-139; (c) T. Vijayakanth; F. Ram; B. Praveenkumar; K. Shanmuganathan; R. Boomishankar, All-Organic Composites of Ferro- and Piezoelectric Phosphonium Salts for Mechanical Energy Harvesting Application. *Chemistry of Materials* 2019**, 31** (15), 5964-5972; (d) C. Jiang; D. W. Stephan, Phosphinimine–borane combinations in frustrated Lewis pair chemistry. *Dalton Trans.* 2013**, 42** (3), 630-637; (e) D. Aguilar; F. Aznárez; R. Bielsa; L. R. Falvello; R. Navarro; E. P. Urriolabeitia, Versatility of Iminophosphoranes and Noninnocent Behavior of the 1,5-Cyclooctadiene Ligand in Palladium(II) Complexes. Synthesis of σ-Allyl Derivatives. *Organometallics* 2007**, 26** (25), 6397-6402; (f) O. Kaufhold; A. Flores-Figueroa; T. Pape; F. E. Hahn, Template Synthesis of Ruthenium Complexes with Saturated and Benzannulated NH,NH-Stabilized N-Heterocyclic Carbene Ligands. *Organometallics* 2009**, 28** (3), 896-901; (g) T. Tannoux; N. Casaretto; S. Bourcier; V. Gandon; A. Auffrant, Reaction of Phosphines with 1-Azido-(2-halogenomethyl)benzene Giving Aminophosphonium-Substituted Indazoles. *J. Org. Chem.* 2021**, 86** (3), 3017-3023.

20. K. Sun; L. Wang; Z.-X. Wang, Synthesis and Characterization of Amido Pincer Complexes of Lithium and Nickel and Catalysis of the Nickel Complexes in the Kumada Cross-Coupling. *Organometallics* 2008**, 27** (21), 5649-5656.

21. (a) D. F. Evans, 400. The determination of the paramagnetic susceptibility of substances in solution by nuclear magnetic resonance. *J. Chem. Soc. Chem. Commun.* 1959**,** (0), 2003-2005; (b) E. M. Schubert, Utilizing the Evans method with a superconducting NMR spectrometer in the undergraduate laboratory. *J. Chem. Educ.* 1992**, 69** (1), 62.

22. (a) F. Speiser; P. Braunstein; L. Saussine, New Nickel Ethylene Oligomerization Catalysts Bearing Bidentate P,N-Phosphinopyridine Ligands with Different Substituents α to Phosphorus. *Organometallics* 2004**, 23** (11), 2625-2632; (b) T. P. A. Cao; S. Labouille; A. Auffrant; Y. Jean; X. F. Le Goff; P. Le Floch, Pd(II) and Ni(II) complexes featuring a "phosphasalen ligand: synthesis and DFT study. *Dalton Trans.* 2011**, 40**, 10029-10037.

23. J.-C. Hierso; A. Fihri; V. V. Ivanov; B. Hanquet; N. Pirio; B. Donnadieu; B. Rebière; R. Amardeil; P. Meunier, "Through-Space" Nuclear Spin−Spin JPP Coupling in Tetraphosphine Ferrocenyl Derivatives: A 31P NMR and X-ray Structure Correlation Study for Coordination Complexes. *J. Am. Chem. Soc.* 2004**, 126** (35), 11077-11087.

24. (a) V. Srinivas; Y. Nakajima; W. Ando; K. Sato; S. Shimada, (Salicylaldiminato)Ni(ii)-catalysts for hydrosilylation of olefins. *Catal. Sci. Techno.* 2015**, 5** (4), 2081-2084; (b) J. Mathew; Y. Nakajima; Y. K. Choe; Y. Urabe; W. Ando; K. Sato; S. Shimada, Olefin hydrosilylation catalyzed by cationic nickel(ii) allyl complexes: a non-innocent allyl ligand-assisted mechanism. *Chem. Commun.* 2016**, 52** (40), 6723-6726; (c) X. Wu; G. Ding; W. Lu; L. Yang; J. Wang; Y. Zhang; X. Xie; Z. Zhang, Nickel-Catalyzed Hydrosilylation of Terminal Alkenes with Primary Silanes via Electrophilic Silicon–Hydrogen Bond Activation. *Org. Lett.* 2021**, 23** (4), 1434-1439.

25. (a) L. Benítez Junquera; M. C. Puerta; P. Valerga, R-Allyl Nickel(II) Complexes with Chelating N-Heterocyclic Carbenes: Synthesis, Structural Characterization, and Catalytic Activity. *Organometallics* 2012**, 31** (6), 2175-2183; (b) I. Hossain; J. A. R. Schmidt, Cationic Nickel(II)-Catalyzed Hydrosilylation of Alkenes: Role of P, N-Type Ligand Scaffold on Selectivity and Reactivity. *Organometallics* 2020**, 39** (18), 3441-3451; (c) T. Hashimoto; K. Shiota; T. Ishimaru; Y. Yamaguchi, Hydrosilylation of Alkenes Using a Hydrosiloxane as a Surrogate for Me2SiH2 and Catalyzed by a Nickel-Pincer Complex. *Eur. J. Org. Chem.* 2021**, 2021** (39), 5449-5452; (d) A. S.-M. Chang; K. E. Kawamura; H. S. Henness; V. M. Salpino; J. C. Greene; L. N. Zakharov; A. K. Cook, (NHC)Ni(0)-Catalyzed Branched-Selective Alkene Hydrosilylation with Secondary and Tertiary Silanes. *ACS Catal.* 2022**, 12** (18), 11002-11014; (e) A. Das; J. Schleinitz; L. Karmazin; B. Vincent; N. Le Breton; G. Rogez; A. Guenet; S. Choua; L. Grimaud; M. Desage-El Murr, A Single Bioinspired Hexameric Nickel Catechol–Alloxazine Catalyst Combines Metal and Radical Mechanisms for Alkene Hydrosilylation. *Chem. Eur. J.* 2022**, 28** (35), e202200596.

26. C. L. Rock; R. J. Trovitch, Anti-Markovnikov terminal and gem-olefin hydrosilylation using a κ4-diimine nickel catalyst: selectivity for alkene hydrosilylation over ether C–O bond cleavage. *Dalton Trans.* 2019**, 48** (2), 461-467.

27. I. Buslov; J. Becouse; S. Mazza; M. Montandon-Clerc; X. Hu, Chemoselective Alkene Hydrosilylation Catalyzed by Nickel Pincer Complexes. *Angew. Chem. Int. Ed.* 2015**, 54** (48), 14523-14526.

28. L. P. Bheeter; M. Henrion; L. Brelot; C. Darcel; M. J. Chetcuti; J.-B. Sortais; V. Ritleng, Hydrosilylation of Aldehydes and Ketones Catalyzed by an N-Heterocyclic Carbene-Nickel Hydride Complex under Mild Conditions. *Adv. Synth. Catal.* 2012**, 354** (14-15), 2619-2624.

29. J. Antonio Fernández; J. Manuel García; P. Ríos; A. Rodríguez, Hydrosilylation of Carbonyl Compounds Catalyzed by a Nickel Complex Bearing a PBP Ligand. *Eur. J. Inorg. Chem.* 2021**, 2021** (29), 2993-2998.

30. B. L. Tran; M. Pink; D. J. Mindiola, Catalytic Hydrosilylation of the Carbonyl Functionality via a Transient Nickel Hydride Complex. *Organometallics* 2009**, 28** (7), 2234-2243.
31. (a) S. Chakraborty; J. A. Krause; H. Guan, Hydrosilylation of Aldehydes and Ketones Catalyzed by Nickel PCP-Pincer Hydride Complexes. *Organometallics* 2009**, 28** (2), 582-586; (b) C. L. Rock; T. L. Groy; R. J. Trovitch, Carbonyl and ester C–O bond hydrosilylation using κ4-diimine nickel catalysts. *Dalton Trans.* 2018**, 47** (26), 8807-8816.
32. L. Postigo; B. Royo, N-Heterocyclic Carbene Complexes of Nickel as Efficient Catalysts for Hydrosilylation of Carbonyl Derivatives. *Adv. Synth. Catal.* 2012**, 354** (14-15), 2613-2618.
33. A. Kumar; R. Gupta; G. Mani, PCP Pincer Carbene Nickel(II) Chloride, Hydride, and Thiolate Complexes: Hydrosilylation of Aldehyde, Ketone, and Nitroarene by the Thiolate Complex. *Organometallics* 2023**, 42** (8), 732-744.
34. N. A. Eberhardt; H. Guan, Nickel Hydride Complexes. *Chem.l Rev.* 2016**, 116** (15), 8373-8426.
35. (a) L.-C. Liang; P.-S. Chien; P.-Y. Lee, Phosphorus and Olefin Substituent Effects on the Insertion Chemistry of Nickel(II) Hydride Complexes Containing Amido Diphosphine Ligands. *Organometallics* 2008**, 27** (13), 3082-3093; (b) J. A. Hatnean; R. Beck; J. D. Borrelli; S. A. Johnson, Carbon−Hydrogen Bond Oxidative Addition of Partially Fluorinated Aromatics to a Ni(PiPr3)2 Synthon: The Influence of Steric Bulk on the Thermodynamics and Kinetics of C−H Bond Activation. *Organometallics* 2010**, 29** (22), 6077-6091; (c) R. B. Lansing; K. I. Goldberg; R. A. Kemp, Unsymmetrical RPNPR' pincer ligands and their group 10 complexes. *Dalton Trans.* 2011**, 40** (35), 8950-8958; (d) M. Kreye; M. Freytag; P. G. Jones; P. G. Williard; W. H. Bernskoetter; M. D. Walter, Homolytic H_2 cleavage by a mercury-bridged Ni(i) pincer complex [{(PNP)Ni}$_2${μ-Hg}]. *Chem. Commun.* 2015**, 51** (14), 2946-2949; (e) S. Murugesan; B. Stöger; M. Weil; L. F. Veiros; K. Kirchner, Synthesis, Structure, and Reactivity of Co(II) and Ni(II) PCP Pincer Borohydride Complexes. *Organometallics* 2015**, 34** (7), 1364-1372; (f) Q. J. Bruch; A. J. M. Miller, A bis(arylphosphinito)amide pincer ligand that binds nickel forming six-membered metallacycles. *Polyhedron* 2020**, 179**, 114380.
36. C. M. Macaulay; S. J. Gustafson; J. T. Fuller, III; D.-H. Kwon; T. Ogawa; M. J. Ferguson; R. McDonald; M. D. Lumsden; S. M. Bischof; O. L. Sydora; D. H. Ess; M. Stradiotto; L. Turculet, Alkene Isomerization–Hydroboration Catalyzed by First-Row Transition-Metal (Mn, Fe, Co, and Ni) N-Phosphinoamidinate Complexes: Origin of Reactivity and Selectivity. *ACS Catal.* 2018**, 8** (11), 9907-9925.
37. C. Zhang; S. D. Grumbine; T. D. Tilley, Reactions of the ruthenium silylene derivative [(η^5-C_5Me_5)(PMe_3)$_2$$RuSiPh_2$(NCMe)]$BPh_4$ with alcohols, ketones and acetic acid. *Polyhedron* 1991**, 10** (11), 1173-1176.
38. R. N. Perutz; S. Sabo-Etienne, The σ-CAM Mechanism: σ Complexes as the Basis of σ-Bond Metathesis at Late-Transition-Metal Centers. *Angew. Chem. Int. Ed.* 2007**, 46** (15), 2578-2592.
39. J. H. Docherty; J. Peng; A. P. Dominey; S. P. Thomas, Activation and discovery of earth-abundant metal catalysts using sodium tert-butoxide. *Nature Chem.* 2017**, 9** (6), 595-600.
40. M. J. Frisch; G. W. Trucks; H. B. Schlegel; G. E. Scuseria; M. A. Robb; J. R. Cheeseman; G. Scalmani; V. Barone; G. A. Petersson; H. Nakatsuji; X. Li; M. Caricato; A. V. Marenich; J. Bloino; B. G. Janesko; R. Gomperts; B. Mennucci; H. P. Hratchian; J. V. Ortiz; A. F. Izmaylov; J. L. Sonnenberg; Williams; F. Ding; F. Lipparini; F. Egidi; J. Goings; B. Peng; A. Petrone; T. Henderson; D. Ranasinghe; V. G. Zakrzewski; J. Gao; N. Rega; G. Zheng; W. Liang; M. Hada; M. Ehara; K. Toyota; R. Fukuda; J. Hasegawa; M. Ishida; T. Nakajima; Y. Honda; O. Kitao; H. Nakai; T. Vreven; K. Throssell; J. A. Montgomery Jr.; J. E. Peralta; F. Ogliaro; M. J. Bearpark; J. J. Heyd; E. N. Brothers; K. N. Kudin; V. N. Staroverov; T. A. Keith; R. Kobayashi; J. Normand; K. Raghavachari; A. P. Rendell; J. C. Burant; S. S. Iyengar; J. Tomasi; M. Cossi; J. M. Millam; M. Klene; C. Adamo; R. Cammi; J. W. Ochterski; R. L. Martin; K. Morokuma; O. Farkas; J. B. Foresman; D. J. Fox *Gaussian 16 Rev. C.01*, Wallingford, CT, 2016.
41. G. Sheldrick, SHELXT - Integrated space-group and crystal-structure determination. *Acta Crystallogr. Sect. A* 2015**, 71** (1), 3-8.
42. O. V. Dolomanov; L. J. Bourhis; R. J. Gildea; J. A. K. Howard; H. Puschmann, OLEX2: a complete structure solution, refinement and analysis program. *J. Appl. Crystallogr.* 2009**, 42** (2), 339-341.
43. L. J. Farrugia *ORTEP-3 program*, Department of Chemistry, University of Glasgow: 2001.
44. Y. Zhao; D. G. Truhlar, The M06 suite of density functionals for main group thermochemistry, thermochemical kinetics, noncovalent interactions, excited states, and transition elements: two new functionals and systematic testing of four M06-class functionals and 12 other functionals. *Theo. Chem. Acc.* 2008**, 120** (1), 215-241.
45. (a) T. H. Dunning Jr.; P. J. Hay, Modern Theoretical Chemistry. In *Modern Theoretical Chemistry*, III, H. F. S., Ed. Plenum: New York, 1977; pp 1-28; (b) P. J. Hay; W. R. Wadt, Ab initio effective core potentials for molecular calculations. Potentials for the transition metal atoms Sc to Hg. *J. Chem.l Phys.* 1985**, 82** (1), 270-283.
46. F. Weigend; R. Ahlrichs, Balanced basis sets of split valence, triple zeta valence and quadruple zeta valence quality for H to Rn: Design and assessment of accuracy. *Phys. Chem. Chem. Phys.* 2005**, 7** (18), 3297-3305.